SHIMADZU

NEWS

Solutions for Science since 1875

A good communicator: The new TOC-4200

Kaizen for maximum performance: *Nexera* in continuous improvement

Glass on the road increases driving safety: Particle measurement of glass beads

Almost omnipresent: Determination of bisphenol A in plastic packaging

1/2012

The new process generation: TOC-4200

IMPRINT

Shimadzu NEWS, Customer Magazine of Shimadzu Europa GmbH, Duisburg

Publisher:
Shimadzu Europa GmbH
Albert-Hahn-Str. 6-10 · D-47269 Duisburg
Phone: +49 - 203 - 76 87-0
Telefax: +49 - 203 - 76 66 25
shimadzu@shimadzu.eu
www.shimadzu.eu

Editorial Team:
Uta Steeger · Phone: +49 - 203 - 76 87-410
Ralf Weber, Tobias Ohme

Design and Production:
m/e brand communication GmbH GWA
Düsseldorf

Circulation:
German: **7,670** · English: **21,850**

A good commun

Figure 1: TOC-4200

Low maintenance and independent operation as well as fast determination of TOC values – these are key features of today's TOC process analyzers. These requirements have been implemented in the new TOC-4200 system. It is used for continuous monitoring of organic carbon pollution in a wide range of applications.

Low-maintenance analyzer

The TOC-4200 is a powerful analyzer that applies catalytic combustion at 680 °C. This temperature is below the melting point of sodium chloride, preventing deactivation of the active centers of the catalyst by a melt.

Use of a platinum catalyst ensures complete conversion of organic carbon compounds to CO_2. The highly sensitive NDIR detector allows small injection volumes (typically 20 – 50 µL), keeping the absolute sample salt load on the catalyst low. A further reduction can be attained with the integrated dilution function, which considerably extends the lifetime of the catalyzer and the associated maintenance intervals. The integrated dilution function not only enables a measuring range up to 20,000 mg/L, but also helps in the creation of multi-point calibrations (max. five calibration points).

By default, TOC is determined by the NPOC method (removing inorganic carbon prior to injection). Depending on the application, users can also work with the difference method (TOC = TC – IC) or the addition method (TOC = NPOC + POC).

New design and software simplify operation

The new design includes spatial separation of electronic components, measuring system and fluids. For filling of standard solutions and hydrochloric acid, the main instrument can now remain closed. The instrument is operated via a color touch-screen. The clear menu navigation simplifies the creation of calibration curves and measurement methods.

icator The new TOC-4200

A calendar function helps in planning automated determination of control samples or calibration curves. Measurement of offline samples is possible without having to stop the instrument. Online measurement is interrupted only as long as the offline sample is being measured. After completion, online measurement resumes automatically.

New communication possibilities

In a chemical industry park, the distance to the process analyzers can be long and it is therefore important that the instruments can be controlled from a control room. Numerous alarm and status signals facilitate the detection of exceeded limit values or maintenance need. The remote function enables users to start measurement or calibration and to select a particular measurement stream. Until now, a separate circuit was needed for each individual control or measurement function. Through the use of bidirectional serial communication, all of these functions can now be implemented via a two-wire bus. By default, the instrument runs under the Modbus protocol. Additional protocols can however be programmed optionally. Moreover, it is possible to query measurement values and the instrument status via a web interface.

Sample preparation

An analysis system is only as good as the sample preparation. The TOC-4200 series features several sample preparation systems that can be optimally adapted to the application range.

In the single stream option, the sample passes through a filter into the sample chamber. A rotating knife then homogenizes the sample before it is transferred to the instrument for analysis. In this way, even samples containing large amounts of particulate matter can be measured without difficulty. After sampling, the chamber and the filter are cleaned using rinse water. Depending on the application, the rinse water can be acidified to prevent the growth of algae.

When multiple sample streams are being measured with one instrument, the multi-sample stream unit (Figure 3) is used. Again, the sample is homogenized prior to analysis. The rinsing function prevents carry-over effects when changing sample streams. The measuring program can be selected individually for each sample stream. The user can also freely determine the measurement sequence of the sample streams.

Figure 2: Straightforward operation via touch-screen

Various options extend the application range

The TN option allows simultaneous determination of TOC and TN_b (total nitrogen) within a few minutes. The measurement sample is injected onto the catalyst at 720 °C. Carbon compounds are then converted to CO_2 and nitrogen compounds to NO. After drying, the carrier gas containing both components first reaches the NDIR detector (where carbon dioxide is detected) and subsequently the chemiluminescence detector. With the help of ozone, a chemiluminescence reaction takes place which is then measured. The peaks of both components are integrated independently and the concentration is calculated.

For continuous TOC analysis of samples with high salt loads (> 10 g/L), Shimadzu has developed a salt kit. The combustion tube has a special shape and two different catalyst spheres are used. This combination significantly extends maintenance intervals. Using this kit in a seawater application, the lifetime of the catalyst and the combustion tube could be increased by a factor of ten.

When monitoring cooling water or condensate systems, the TOC contents are generally much lower. Here, the high-sensitivity kit for measuring TOC concentrations below 1 mg/L will be helpful.

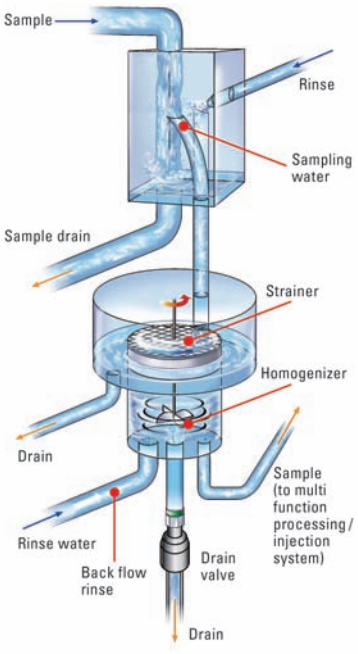

Figure 3: Sampling unit with homogenization

Prototype has passed operational reliability test

A prototype of the TOC-4200 was tested in a German chemical park during a three-month trial under real conditions. The sample was a high salt concentration wastewater. Thanks to the special combustion tube and catalyst filling of the salt kit, the TOC-4200 did not need any maintenance. In addition, its excellent performance and ease of use was clearly demonstrated.

Caviar and ciga

FTIR-ATR analysis of alginate on ci

Figure 1: Alginate based Caviar prepared with fluoresceine excited with analytical wavelength of 460 nm in a Shimadzu fluorescence spectrophotometer RF-5301PC: it is fluorescent caviar filled into a 1 cm quartz cell

We will gladly send you additional information. Please enter the corresponding number on the reply card or order via Shimadzu's News App or News WebApp.
Info 401

According to estimations (European Commission standardization mandate, M/425), carelessly unattended cigarettes cause some 14.000 fires every year in the EU, with 7,000 fatalities, 2,500 injuries and around 50 million euro of material damage. How can molecular gastronomy decrease the number of these accidents?

Spherification is one of many applications of molecular gastronomy which combine unconventional textures and flavors. It's a process of turning liquid juice into juice-filled pearls. To produce these pearls some alginate – a substance derived from algae – is simply dissolved in a juice. Droplets of the juice are then dropped into a calcium water bath. The calcium from the water bath reacts immediately with the alginate in the juice to form a film around the droplet. Spheres of juice are thus created which look just like caviar (Figure 1). How is fake caviar related to cigarettes?

Fake caviar and its relationship to cigarettes

Cigarettes are a source of heat and therefore represent a fire hazard. They can ignite materials such as furniture or textiles. Self-extinguishing cigarettes can reduce the number of accidents compared to unattended cigarettes. These cigarettes are produced by adding two special retardant bands to the cigarette paper during manufacturing.

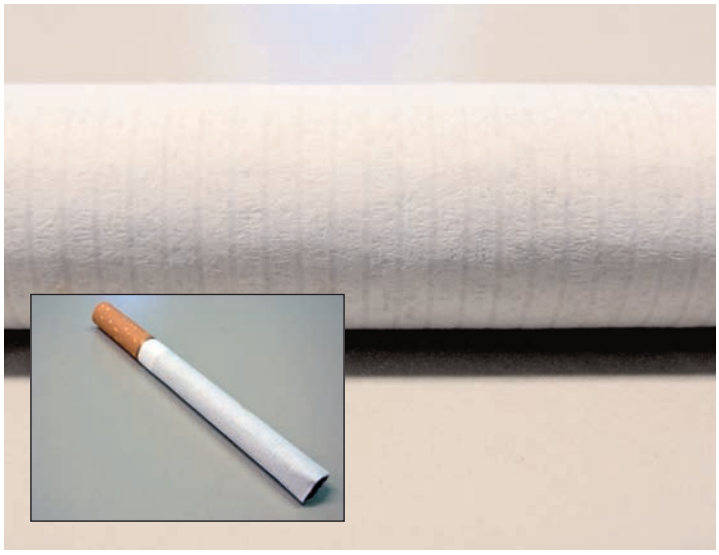

Figure 2: View of a cigarette and zoom onto one form of the cigarette paper. In this case the rings which help to burn the cigarette continuously are apparent.

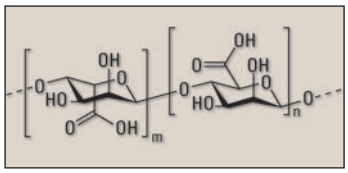

Figure 3: Structure of alginate acid base of the sodium alginate salt

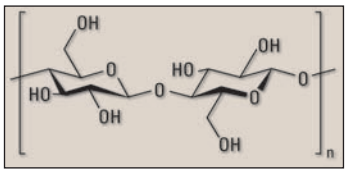

Figure 4: Structure of a common cellulose molecule

rettes

garette paper

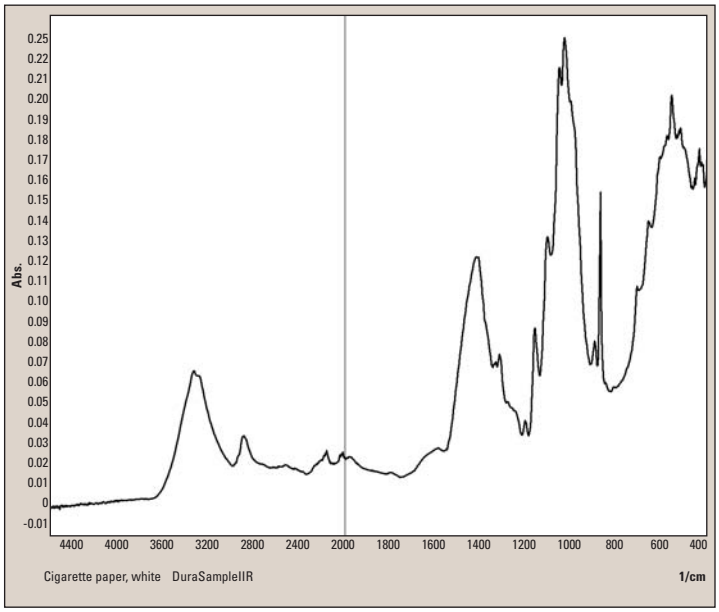

Figure 5: Infrared spectrum of a white cigarette paper measured with single reflection technique

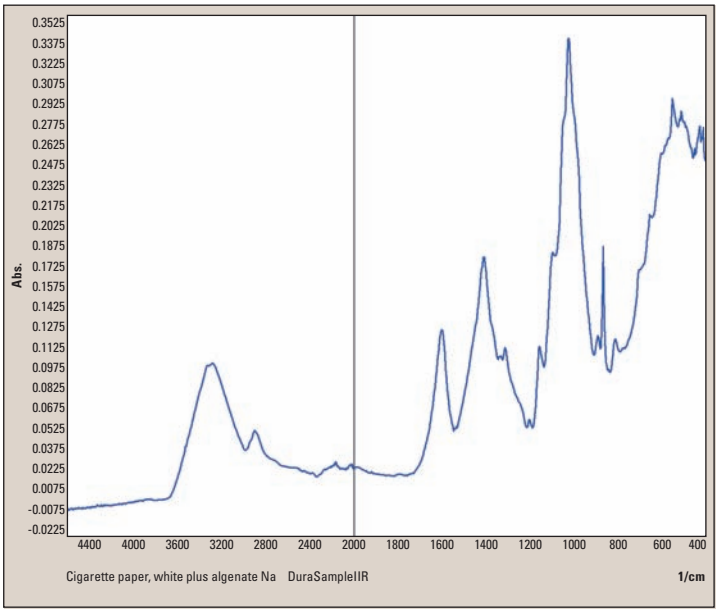

Figure 6: Infrared spectrum of cigarette paper with a thin layer of Sodium-Alginate, surface analysis with single reflection ATR technique

These bands act as speed bumps by decreasing the flow of oxygen through the paper to the burning tobacco. They slow down the rate at which the cigarette burns as the lit end crosses over. They are more likely to self-extinguish. These speed bumps are made of a layer of alginate on the cigarette paper – the same alginate used for the molecular caviar.

A simple application of the FTIR spectrophotometer in combination with the single reflection unit demonstrates the differences of the materials. The single material spectra and the spectrum of the final paper layer are shown step by step. All significant components such as cellulose in the paper, sodium carbonate and alginate have broad signals in the infrared spectrum. All have in common the polysaccharide characteristics of the 6 ring structure in conjunction with -C-O-C- and the -OH bonded groups.

The paper spectrum shows significant signals for the whitener of the sodium carbonate. These are a sharp signal at 700, at 900 and a broad signal at 1400 cm^{-1}. This is reasonable based on the substructure of the carbonate group which generates two $-CO^-$ and one -C=O bonding constellation and also distribution of electrons over this bonding system, resulting in the broad signal at 1400 cm^{-1}. In the literature, the symmetric valence vibration ϑsy ($-COO^-$) is calculated as 1440 - 1360 cm^{-1}.

The spectrum of alginate on paper shows a mixture of alginate and paper. It is possible to differentiate between both spectra. Even though both materials are based on polysaccharide, they have differences in their molecular structure which are visible in the infrared spectrum. The signal at 1600 cm^{-1} is the -OH bonding in the huge molecules. When comparing the structure of the polysaccharides the different positioning at the ring systems generates the additional signal in comparison to the cellulose.

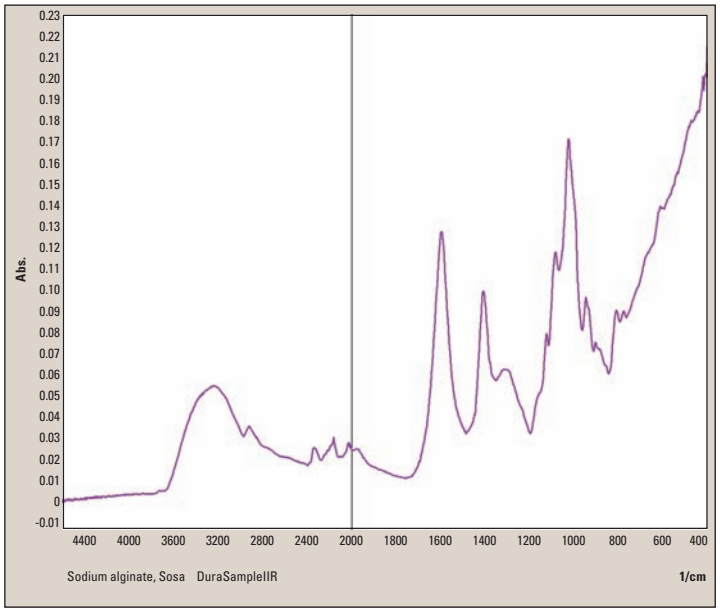

Figure 7: Infrared Spectrum of sodium alginate powder measured with single reflection technique

Finding new antibiotic s

LC-IT-TOF-MS of alkylated neomycin antibiotics

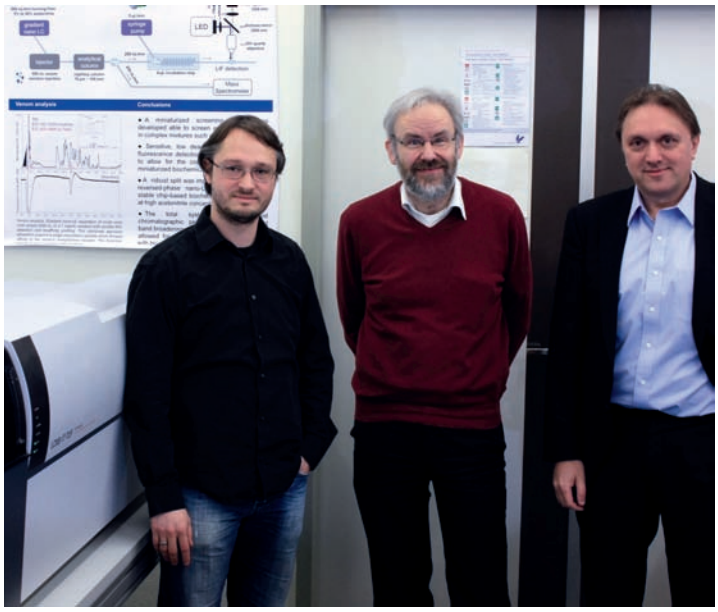

From left to right: Dr. Martin Giera, Prof. Dr. Wilfried M.A. Niessen, Prof. Dr. Hubertus Irth

Dr. Martin Giera and Prof. Dr. Wilfried M.A. Niessen
VU University Amsterdam,
Faculty of Sciences,
BioMolecular Analysis Group,
De Boelelaan 1083,
1081 HV Amsterdam,
The Netherlands

Structural elucidation of small molecules is an integral part of numerous life-science areas. Although NMR spectroscopy undoubtedly plays the most important role in the elucidation of analyte structures, mass spectrometry (MS) has become widely applied in structural elucidation wherever possible. The success of MS based structural elucidation is based on several facts:

a) compared to NMR, only small amounts of the analyte are necessary
b) the technique can conveniently be coupled on-line to chromatography based separations (LC or GC)
c) more and more knowledge has been gained in the last decade about the fragmentation mechanisms of particular analyte classes, i.e. sugars, peptides or DNA/RNA molecules. The possibility to perform MS/MS or MS^n experiments combined with high resolution MS instruments has especially been crucial for this development.

The following example shows the significance of the combination of LC-MS^n capabilities and high-resolution spectral data with a Shimadzu LC-IT-TOF-MS instrument.

Case study

Finding new antibiotic substances is a key challenge as microorganisms are becoming ever more resistant to currently available treatments. Enhanced screening and identification techniques for bioactive substances from diverse sources therefore have to be developed and applied. At the VU University Amsterdam, on-line screening strategies are developed which can be combined with LC to assess bioactivity. In this case, the effect of single alkylation of neomycin at its different nitrogen atom sites on the antibacterial behavior of the formed derivative has been investigated [1]. The reductive alkylation of the aminoglycoside antibiotic neomycin with one equivalent n-octanal leads to the formation of six regioisomers (Fig. 1).

The regioisomers were separated by reversed-phase LC, and differences in their antibacterial behavior were demonstrated [1]. In order to elucidate the compound structures an IT-TOF instrument coupled to LC was applied. A schematic overview of the system is shown in figure 2.

Hi-res MS data used for the molecular formula

In the first instance, all regioisomers displayed the same m/z value of 727.4448. This proved that the mono-alkylation actually worked. The performance of MS/MS still yielded identical fragment ions with m/z 564.3628 for all six regioisomers, rendering the different species so far indistinguishable. In MS^3, the first differences between the six regioisomers could be obtained. At this stage, it could be deduced which of the three rings was alkylated. While a ring-4 alkylation caused two fragments with m/z 273.217 and 405.261, a ring-2 alkylation gave a fragment with m/z 275.233, and a ring-1 alkylation resulted in the formation of two fragments with m/z 273.217 and 435.317.

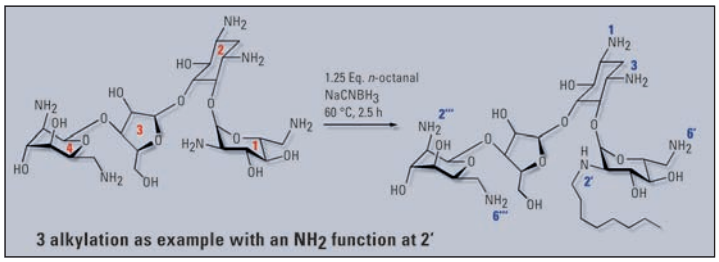

Figure 1: Reductive alkylation of neomycin. The alkylated derivatives have a single n-octyl chain on one of the six nitrogen atoms, as exemplified for N-2. Ring numbers (in the ring) and nitrogen numbers are specified.

ubstances

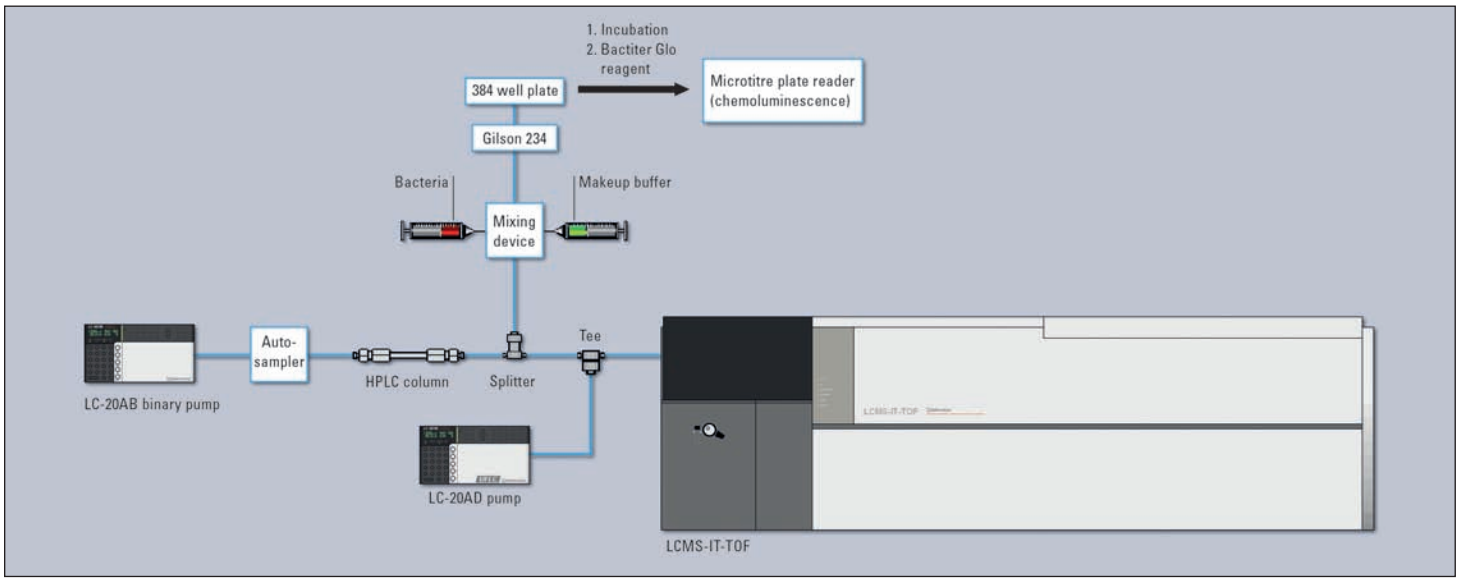

Figure 2: Schematic overview of the LC–IT-TOF-MS setup used in this study

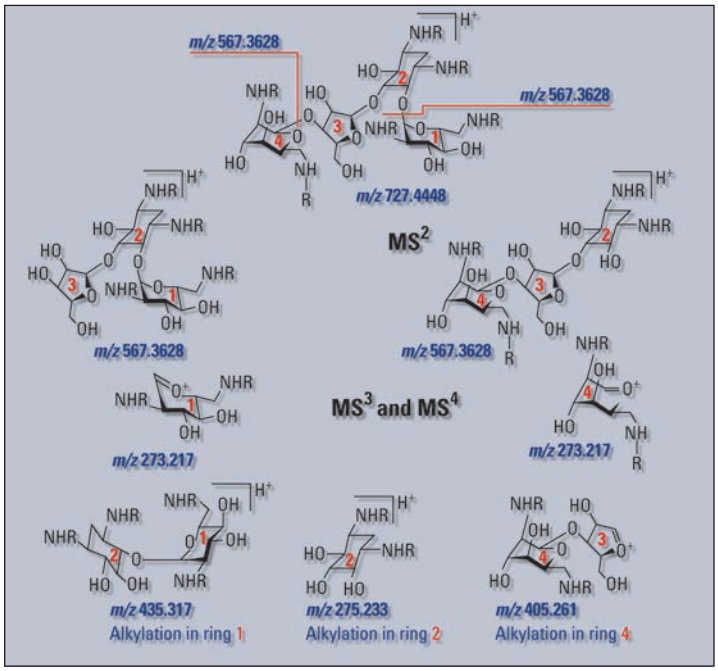

Figure 3: Fragmentation scheme of mono-N-alkyl neomycin derivatives in MS^n experiments, showing the different ring losses and the calculated m/z values of the resulting fragmentions. R = n-octyl or H.

In summary: high resolution MS data allowed generation of the molecular formulae for the substances formed. MS/MS fragmentation, as would also be available on a Q-TOF instrument, resulted in the loss of one of the (unmodified) terminal aminosugars, thereby providing no insights into the molecular structures. MS^3 experiments performed on the identical MS/MS fragments provided the first structural insights: it enabled assigning of the ring number at which alkylation took place. A summary of the fragmentation path up to MS^3 is shown in figure 3.

The final question to answer was: which nitrogen atom in the ring was alkylated? MS^4 experiments on the fragment ion with m/z 275.233 (ring-2 alkylation) resulted in identical spectra, as expected due to the symmetrical structure of the N-1 and N-3 derivatives. For the other four regioisomers, MS^4 experiments did lead to characteristic fragment ions and subsequently unequivocal assignment of the alkylated ring nitrogen atom.

Conclusion

High-resolution MS^n experiments on an LC-IT-TOF-MS instrument can lead to a full structural assignment of closely related compounds. The assignment of the alkylated ring in the N-octyl neomycin derivatives was accomplished by investigating the subsequent cleavages of the glycosidic bonds. MS^4 experiments were needed to fully assign the structures of four out of the six regioisomers. To assign the other two, preparative LC and subsequent NMR analysis would be needed.

[1] Giera M et al. Rapid Commun Mass Spectrom, 2010, 24:1439

Kaizen for maximum pe

Nexera in continuous improvement

Figure 1: *Nexera* pump with installed quaternary gradient valve

Kaizen is the Japanese philosophy of life and work that strives for continuous improvement. In the business world, Kaizen stands for continuous improvement processes. Every product and process has the opportunity for improvement – even those which are said to be the optimal solution.

For Shimadzu's *Nexera* system, Kaizen means that 18 months after its first launch, a series of modifications and new solutions increases the applicability of the *Nexera* family.

The quaternary gradient option has already been introduced and the flow range has been increased to a maximum of 10,000 mL/min. This has extended the range of use involving pumps for solvent mixing and semi preparative applications.

To ensure that the pumps work reliably as the backbone of the system, modifications have been made to the pump head, piston suspension and valves. While mostly not visible to the user, the reduced air bubble sensitivity and the improved lifetime are remarkable.

It's all in the right mix

Gradient reproducibility and accuracy are crucial when fast gradients are applied to short columns. This requires as 'perfect' as possible choice of the most appropriate components of the mobile phase. The micro-reactors used so far with 20 µL and 180 µL (TFA version) have meanwhile been supplemented by a 40 µL and 100 µL version and the design of the 180 µL micro-reactor has been optimized to minimize baseline fluctuations caused by mixing. More choices, however, mean more 'difficult' decisions for the user as to which mixing volume represents the optimal solution for a specific application.

Autosampler as heart of the system

The heart of the Nexera system is and will be the autosampler. Fast and carryover-free injections have repeatedly been emphasized as its essential characteristics. In terms of changes, the major focus is on durability and maintenance-free operation, without overriding existing features or compromising performance.

Many laboratories already use the possibility to inject larger sample volumes. When installing a larger sample loop (max. 2.000 µL) in the system, it is possible to inject these larger volumes. However, flow rate, pressure range and column dimensions must be taken into account to prevent damage to the system and/or the column.

Depending on the application, the use of fixed sample loops is worth considering. System volume is reduced, resulting in shorter gradient run times and shorten equilibration time between the analyses. Considering about peak symmetry many advantages speak for this injection principle. One important point still remains, when talking about possible carryover from sample to sample: the user shall decide about the priorities for his/her application and system, as a generic answer cannot be given.

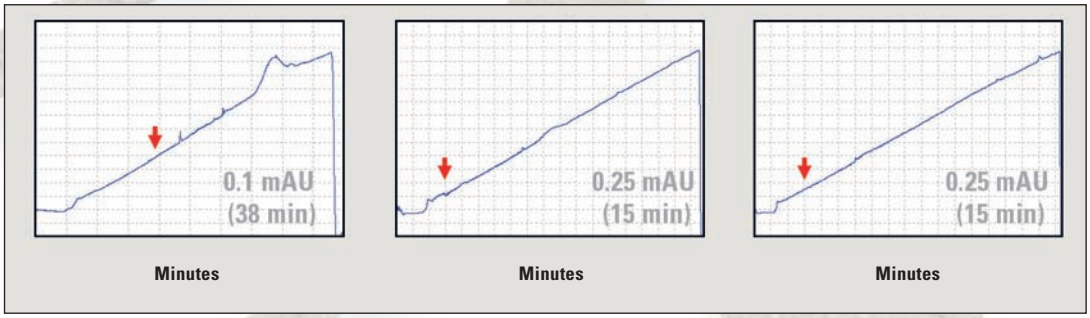

Figure 2 a-c: performance test of the new 180 µL micro-reactor at (gradient A: 0.1 % TFA in water, B: 0.1 % TFA in acetonitrile, C: 0 - 45 % B

rformance

New detector cells

Detectors are the eyes of the system. Standard and semi-micro flow cells are supplemented by cells with higher sensitivity. These cells can be considered as midfield between the former two with respect to cell volume. A longer optical path compared to the semi-micro cell and a reduced diameter of the beam path compared to the standard cell in combination with stronger focusing, allow greater sensitivity. Two additional cells are available for the UV detector and one additional cell is available for the photodiode-array detector.

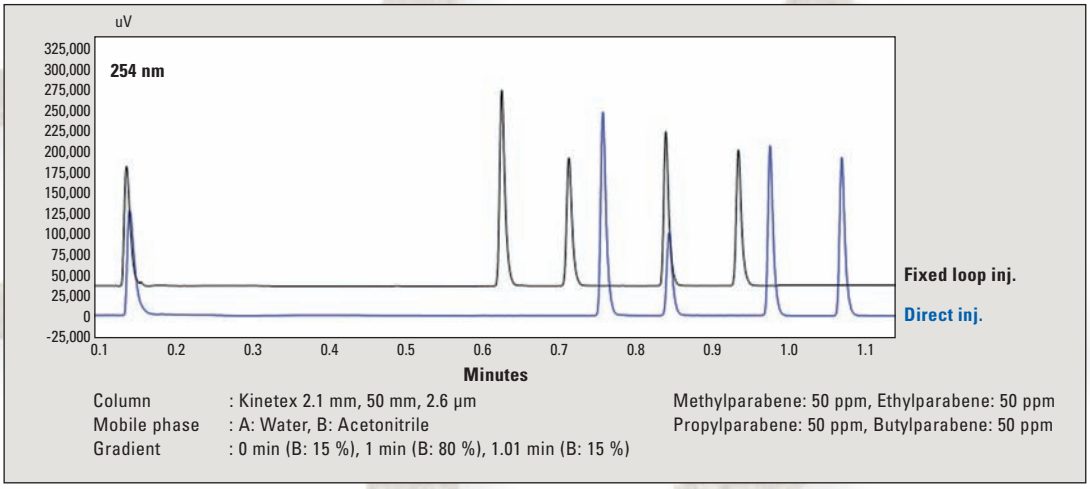

Figure 3: Comparison of direct injection with loop injection

What is the optimal flow cell for a particular application? The *Nexera* system guide supplied with the system can provide an initial answer. Even if the new flow cells are not yet specified, users are provided with a guideline stating which cell under which conditions would be the optimum choice.

"Kaizen", continuous improvement – this process will continue ...

改善

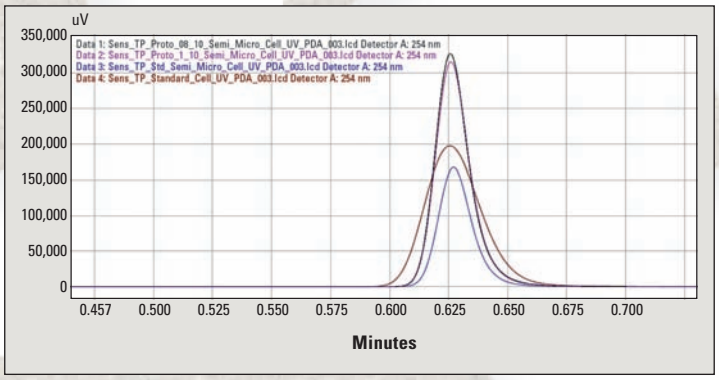

Figure 4: Comparison of the peaks obtained using the new flow cells versus the semi-micro flow cell

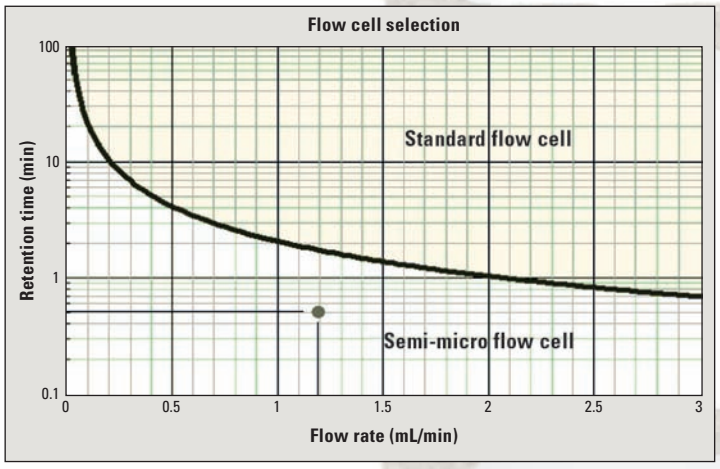

Figure 5: Flow cell selection diagram from the Nexera system guide

SQTs – excellent candidates pre infections and cancer?

Biological activitie products rich in t

	BC	ST	STI	SE	CD	EC	PA	PAI	PF	SA	SAI
Cabreuva oil	–	–	–	–	–	–	–	–	–	–	–
Cedarwood oil	13.5	18.5	19	16.5	–	8	–	–	–	6	6
Juniper berry oil	12.5	16	16.5	14.5	7	8	–	–	–	9	9
Myrrh oil	13.5	22	24	21	6	10	–	–	–	9	10
α-Bisabolol	12.5	18	17.5	16.5	7	9	–	–	–	9	9
Cedrol	13	15	16	14	–	6	–	–	–	7	7
(E,E)-Farnesol	11	13	14	14	9	8	–	–	–	–	–
(E)-Nerolidol	11	23	21	22	–	10	–	–	–	–	–
(Z)-Nerolidol	11.5	24	21.5	22	–	11	–	–	–	–	–
Sabinene	12	18	18	16.5	6	8	–	–	–	–	–
Thujopsene	10.5	14	16.5	15	–	6	–	–	–	9	10

Table 1: **Antimicrobial activity I** – Inhibitory zones [mm] in agar diffusion assay

Sabine Krist, Martina Hoeferl, Leopold Jirovetz
Department of Clinical Pharmacy and Diagnostics, University of Vienna, Austria

Volatile organic compounds have been the subject of many investigations. In the last years, there has been a strong research focus on the biological activities of organic volatiles. In this work, data concerning the antimicrobial activity as well as antiviral, anticancer and cytotoxic properties of selected sesquiterpenes and terpenoids (SQTs) and natural products rich in these volatiles is presented.

Antimicrobial tests

For the antimicrobial tests, the agar diffusion disc method and the agar dilution method were applied. These tests were carried out against four strains of Gram-positive and seven strains of Gram-negative bacteria.

At first, the agar diffusion disc method was carried out with 6 mm paper discs and 6 µL of sample. After incubation of the bacteria at 37 °C for 24 h, the diameter of the inhibition zone (IZ) was measured. Afterwards, the agar dilution method was applied.

The test compounds were added to broth containing 1.0 % (v/v) Tween 80 at the appropriate volumes to produce final concentrations of samples in the range of 1 to 1,000 ppm. The concentration of pathogens in the medium exceeded 106 - 107 cfu/cm³. The agar plates were inoculated by pipetting 0.1 mL of the culture and 6 µL of the samples onto paper discs (6 mm) and were then incubated at 37 °C for 24 h.

Tested microorganisms

Gram-positive bacteria

- Bacillus cereus (ATCC 11778) **BC**
- Staphylococcus aureus (ATCC 6538) **ST**
- Staphylococcus aureus (food spoilage isolate) **STI**
- Staphylococcus epidermidis (clinical isolate) **SE**

Gram-negative bacteria

- Citrobacter diversus (clinical isolate) **CD**
- Escherichia coli (ATCC 8739) **EC**
- Pseudomonas aeruginosa (ATCC 9627) **PA**
- Pseudomonas aeruginosa (clinical isolate) **PAI**

	BC	ST	STI	SE	CD	EC	PA	PAI	PF	SA	SAI
Cabreuva oil	0.4	0.4	0.4	0.4	0.8	0.8	0.8	0.8	0.8	0.8	0.8
Cedarwood oil	0.2	0.2	0.2	0.2	0.4	0.4	0.8	0.8	0.8	0.4	0.4
Juniper berry oil	0.2	0.2	0.2	0.2	0.4	0.4	0.8	0.8	0.8	0.4	0.4
Myrrh oil	0.1	0.1	0.1	0.1	0.2	0.2	0.4	0.4	0.4	0.2	0.2
α-Bisabolol	0.1	0.1	0.1	0.1	0.2	0.2	0.4	0.4	0.4	0.4	0.4
Cedrol	0.2	0.2	0.2	0.2	0.4	0.4	0.8	0.8	0.8	0.4	0.4
(E,E)-Farnesol	0.4	0.4	0.4	0.4	0.8	0.8	0.8	0.8	0.8	0.8	0.8
(E)-Nerolidol	0.1	0.1	0.1	0.1	0.2	0.2	0.4	0.4	0.4	0.2	0.2
(Z)-Nerolidol	0.1	0.1	0.1	0.1	0.2	0.2	0.4	0.4	0.4	0.2	0.2
Sabinene	0.4	0.4	0.4	0.4	0.8	0.8	0.8	0.8	0.8	0.4	0.4
Thujopsene	0.2	0.2	0.2	0.2	0.4	0.4	0.8	0.8	0.8	0.4	0.4

Table 2: **Antimicrobial activity II** – MIC [%] in agar serial dilution assay

venting viral

s of selected sesquiterpenes and terpenoids as well as natural hese volatiles

- Pseudomonas fluorescens (food spoilage isolate) **PF**
- Salmonella abony (ATCC 6017) **SA**
- Salmonella abony (clinical isolate) **SAI**

By applying disc diffusion test, the Gram-positive bacteria as well as the Gram-negative bacterium Eschericha coli were inhibited by all essential oils and single compounds tested except cabreuva oil. For the Gram-negative bacteria, Pseudomonas aeruginosa (ATCC 9627 and clinical isolate) and Pseudomonas fluorescens could not be inhibited by any of the tested volatiles. The agar dilution assay, resulting in minimal inhibitory concentration (MIC), revealed that substance concentrations of 0.1 to 0.8 % of the tested volatiles and essential oils were necessary in order to achieve an overall reduction of bacteria. The Minimal Bacterial Concentration (MBC), defined as the lowest concentration of an agent that shows no evidence of microbial growth in the determination assay and which is also achieved by the agar dilution method, was between 0.2 and 1 % for the tested SQTs and essential oils. Detailed results are shown in tables 1-3.

	BC	ST	STI	SE	CD	EC	PA	PAI	PF	SA	SAI
Cabreuva oil	0.8	0.8	0.8	0.8	0.8	0.8	1	1	1	0.8	0.8
Cedarwood oil	0.4	0.4	0.4	0.4	0.8	0.8	0.8	0.8	0.8	0.8	0.8
Juniper berry oil	0.4	0.4	0.4	0.4	0.4	0.4	0.8	0.8	0.8	0.8	0.8
Myrrh oil	0.2	0.2	0.2	0.2	0.4	0.4	0.8	0.8	0.8	0.4	0.4
α-Bisabolol	0.2	0.2	0.2	02	0.4	0.4	0.8	0.8	0.8	0.8	0.4
Cedrol	0.4	0.4	0.4	0.4	0.8	0.8	0.8	0.8	0.8	0.8	0.8
(E,E)-Farnesol	0.8	0.8	0.8	0.8	0.8	0.8	> 0.8	> 0.8	> 0.8	> 0.8	> 0.8
(E)-Nerolidol	0.2	0.2	0.2	0.2	0.4	0.4	0.4	0.4	0.4	0.4	0.4
(Z)-Nerolidol	0.2	0.2	0.2	0.2	0.4	0.4	0.4	0.4	0.4	0.4	0.4
Sabinene	0.4	0.4	0.4	0.4	0.8	0.8	0.8	0.8	0.8	0.8	0.8
Thujopsene	0.4	0.4	0.4	0.4	0.8	0.8	0.8	0.8	0.8	0.8	0.8

Table 3: **Antimicrobial activity III** – MBC [%] in agar serial dilution assay

Antitumor tests

Various organic volatiles were tested for their anti-tumor and antiviral potential, investigated on HeLa (human cervix carcinoma) cells. Jurkat E6.1 (human leukaemic T cell lymphoblast derived from a patient with acute lymphoblastic leukaemia) cells were included in the analyses to account for the possibility of cell-type specific activity of the samples investigated. Cellular toxicity of volatile compounds was tested using the CytoTox-96® assay according to the standard manufacturer's protocol. The ED_{50} values were calculated by regression analysis of the dose response curves generated from the data.

Tested cell lines:

- HeLa (human cervix carcinoma)
- Jurkat E6.1 (human leukaemic T cell lymphoblast)
- Cellular toxicity: Cytotox-96® assay

All SQTs tested affected the viability of HeLa cells. A reduction of 50 % of HeLa cells, growing as a monolayer, was observed after applying nerolidol (natural and synthetic) and (E,E)-farnesol at concentrations (CC_{50}) less than 5 µm. The CC_{50} of synthetic nerolidol in HeLa cells was almost ten times less than the effect dose required to achieve 50 % cytotoxicity of the cells (ED_{50}). A similarity in the activity against tumor cells between nerolidol and farnesol could be attributed to their similar chemical structure. Tables 4 and 5 show detailed results.

Antiviral tests

For virus infections, mouse polyomavirus (MpyV) strain A2 was used at the multiplicity of infection (MOI)5 plaque-forming units per cell. The titer of virus was estimated by immunofluorescence microscopy.

- Tested virus
  mouse polyoma virus (MPyV)
- Infected cells
  3T6 cells (Swiss albino mouse fibroblasts)
- Assay
  plaque reduction assay
- Virus titration
  immunofluorescent staying against early or late viral antigens

Together with a remarkable reduction on the viability of tumor cells, antiviral activity of selected volatile compounds could be demonstrated. The effective concentration (CC_{50}) of natural nerolidol against mouse polyomavirus appeared to be more than ten times lower compared with the cytotoxic dose (ED_{50}), the synthetic nerolidol showed a CC_{50} three times lower compared with the ED_{50} (see table 6).

Cytotoxic tests

Today, little is known of the cytotoxic properties of volatile aroma compounds. The in-vitro cytotoxicity of promising volatiles was evaluated on cell viability of HeLa cells. Curcumin, an active natural anticancer agent and Antimycin D, a well-established anticancer drug, were used as references.

	HeLa		Jurkat	
	CC_{50} (µM)	ED_{50} (µM)	CC_{50} (µM)	ED_{50} (µM)
α-Bisabolol	< 5	< 10	< 20	< 20
β-Caryophyllene	< 15	< 30	–	–
Caryophyllene oxide	< 30	< 50	–	–
Cedrol	< 20	< 20	< 50	–
(E,E)-Farnesol	< 5	< 10	–	–
Farnesol (isomer mix.)	< 10	< 10	–	–
Longifolene	< 30	< 50	–	–
Patchoulol	< 10	< 10	< 10	< 10
Santalol	< 20	< 30	< 50	–
Ylang fraction	< 30	< 50	–	–

Table 4: **Antitumor activity I** – CC_{50} = concentration required to reduce cell number to 50 %; ED_{50} = effective dose required to achieve 50 % cytotoxicity

	HeLa		Jurkat	
	CC_{50} (µM)	ED_{50} (µM)	CC_{50} (µM)	ED_{50} (µM)
Nerolidol (synthetic)	1.5 ± 0.7	< 10	4.2 ± 1.4	< 10
Nerolidol (natural)	4.2 ± 1.4	< 10	–	–
(Z)-Nerolidol	< 5	< 10	–	–
(E)-Nerolidol	< 10	< 10	–	–

Table 5: **Antitumor activity II** – CC_{50} = concentration required to reduce cell number to 50 %; ED_{50} = effective dose required to achieve 50 % cytotoxicity

The cytotoxic activity of volatile compounds within 24 h after the treatment was evaluated using the Cytotoxic Detection Kit. The influence of the tested volatiles on viability of HeLa cells was tested using cell Proliferation Reagent WST-1 after 24 h of incubation.

- Tested cell lines: HeLa (human cervix carcinoma)
- Cellular toxicity and cell lysis: Cytotoxicity Detection Kit (LDH), Roche Diagnostics
- Cell proliferation, growth, viability and chemosensitivity: Cell Proliferation Reagent WST-1, Roche Diagnostics

Among the volatile aroma compounds tested, the sesquiterpen alcohol (Z)-Nerolidol demonstrated the highest cytotoxic activity, comparable to the reference compound curcumin at a concentration of 15 µm. As a possible mechanism of the cytotoxicity of sesquiterpenes a direct interaction with the cell membrane, leading to altered permeability and cell death, is considered. Nerolidoles in particular may act as prospective agents for cancer chemoprevention. The other volatile compounds investigated (α-bisabolol, cedrol, santalol and patchoulol) were sufficient to achieve 50 % of cytotoxicity on the HeLa cell line in comparable concentrations as (Z)-nerolidol. Detailed results are shown in table 7.

GC analysis

A Shimadzu GC-17A with FID and a Shimadzu GCMS-QP5050 were applied for the qualitative and quantitative analysis of natural products rich in sesquiterpenes and terpenoids investigated in this study.

Vistas

The sesquiterpenes and terpenoids (SQTs) caryophyllenes, α-bisabolol, cedrol, farnesol, longifolene, nerolidol, patchoulol, sabinene, santalols, thujopsene as well as natural products (essential oils, oil fractions and oleoresins) rich in these volatiles possess various biological activities. Many of these compounds show antimicrobial properties against selected Gram-positive and Gram-negative bacteria as was demonstrated by applying agar dilution and agar diffusion methods [1,2]. Furthermore, pronounced antiviral, anticancer and cytotoxic properties against mouse polyomavirus infected 3T6 cells and human cancer cell lines were shown [3,4]. SQTs may therefore be excellent candidates in the prevention of viral infections and cancer.

	Antiviral activity	
	CC_{50} (µM)	ED_{50} (µM)
α-Bisabolol	< 10	< 10
Cedrol	< 10	< 5
Patchoulol	< 10	< 5
Santalol	< 20	< 20
Nerolidol (synthetic)	3.2 ± 1.5	11 ± 1.8
Nerolidol (natural)	1.2 ± 0.4	10.6 ± 3

Table 6: **Antitumor activity III** – CC_{50} = concentration required to reduce infected cells to 50 %; ED_{50} = effective dose required to achieve 50 % cytotoxicity

References

[1] E. Schmidt, S. Bail, S.M. Friedl, L. Jirovetz, G. Buchbauer, J. Wanner, Z. Denkova, A. Slavchev, A. Stoyanova and M. Geissler; Antimicrobial Activities of Single Aroma Compounds. Natural Product Communications 5, 1365-1368 (2010).

[2] J. Wanner, E. Schmidt, S. Bail, L. Jirovetz, G. Buchbauer, V. Gochev, T. Girova, T. Atanasova and A. Stoyanova; Chemical Composition and Antimicrobial Activity of Selected Essential Oils and Some of Their Main Components. Natural Product Communications 5, 1359-1364 (2010).

[3] B. Ryabchenko, E. Tulupova, E. Schmidt, K. Wlcek, G. Buchbauer and L. Jirovetz; Investigations of Anticancer and Antiviral Properties of Selected Aroma Samples. Natural Product Communications 3, 1085-1088 (2008).

[4] B. Ryabchenko, E. Tulupova, E. Schmidt, W. Jaeger, G. Buchbauer and L. Jirovetz; Cytotoxic Properties of Selected Sesquiterpene Alcohols on Human Cervix Carcinoma Cell lines. Journal of Essential Oil Bearing Plants 14, 316-319 (2011).

Remarks

In cooperation with Dr. Margit Geissler, Shimadzu Europe GmbH

	Cytotoxic activity	
	CCT_{50} (µM)	CCP_{50} (µM)
α-Bisabolol	39.0 ± 8.0	33.6 ± 6.4
Cedrol	48.3 ± 5.8	40.0 ± 8.1
Patchoulol (80 %)	48.3 ± 14.0	40.6 ± 11.7
Santalol	29.6 ± 2.6	28.8 ± 13.3
(Z)-Nerolidol	16.5 ± 6.7	20.4 ± 7.8
Curcumin	15.0 ± 5.0	18.3 ± 5.7
Actinomycin D	0.17 ± 0.05	0.056 ± 0.027

Table 7: **Cytotoxic activity** – CCT_{50} = concenrtation required to achieve cytotoxicity of 50 %; CCP_{50} = concentration necessary to achieve a decrease in cytoproliferation by 50 %

Light is difficult

Tips for the determination of light elements

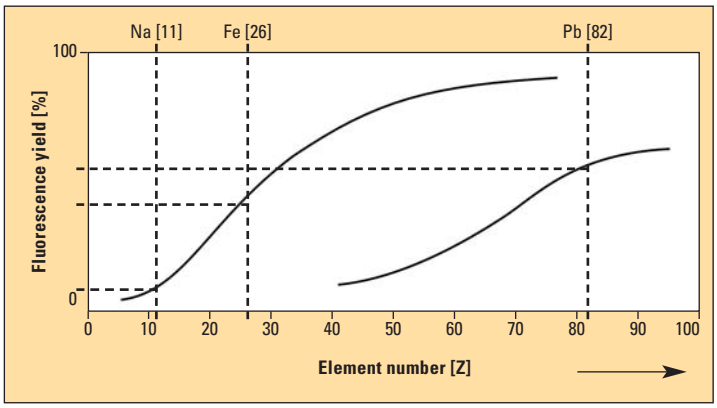

Figure 1: Fluorescence yield as a function of the element number. Lighter elements have a lower yield, heavier elements a higher yield.

X-ray fluorescence analysis is a powerful method in elemental analysis for reliable determination of concentrations in the low ppm-range without sample preparation. In addition, virtually all elements of the periodic table can be measured simultaneously. Results can already be available in less than two minutes.

The measuring range of X-ray fluorescence spectrometers often starts with sodium (Na), sometimes magnesium (Mg) and sometimes only with carbon (C). It is interesting to note that in most cases the heaviest element measurable is always uranium (U).

Why is it so difficult to measure lithium (Li) using an X-ray fluorescence spectrometer? Because it is, in general, more difficult to measure the lighter elements – several challenges need to be mastered.

Detector window

The first challenge is the detector window which often consists of beryllium (Be) and only transmits sufficient radiation of elements equal or heavier than sodium (Na).

For instance, Shimadzu's EDX-800 is capable of carrying out measurements starting from carbon (C) due to the use of a special window sensitive enough to transmit enough radiation from lighter elements.

Air

Air also reduces the amount of fluorescence radiation that hits the detector. In this case, it is helpful to remove air out of the sample compartment. Modern spectrometers, such as the EDX instrument series, offer two options: either the sample compartment is evacuated or it is flooded with helium. Evacuation is practical, simple and can be implemented almost without running costs but is, however, only suitable for solid samples. Liquid samples are measured in a helium atmosphere. In practice, it has proven useful to measure samples, for which the content of aluminum/silicon or lighter elements needs to be determined, under vacuum or helium conditions.

Fluorescence yield

An additional difficulty when measuring lighter elements is the fluorescence yield of these elements. In an X-ray fluorescence spectrometer, the sample is excited with X-rays. The sample, in turn, emits fluorescence radiation – as well X-rays. As this emitted radiation is characteristic for the respective element, its identity as well as its concentration can be determined unequivocally. The fluorescence yield of lighter elements is, however, much lower than that of heavier elements. Sodium will always have a lower fluorescence yield than lead.

Sample vessel

If the sample is transferred to a sample vessel, its base usually consists of a thin polymer film which is highly transparent to X-rays. But caution is required as well. There are various films that differ in their resistance to chemicals, but also in their degree of transparency. Mylar is often used as standard film due to its good chemical resistance. When Mylar is used for the measurement of aqueous sodium solutions, however, sodium may not be included in the analytical results. The transparency of Mylar with respect to X-rays is indeed good. For the case described here it is appropriate to use Ultralene instead of Mylar, as its transparency is much higher.

When an X-ray system, such as Shimadzu's EDX instrument series, offers sophisticated features such as special windows and helium or vacuum options, the tips mentioned above will enable simple measurement of light elements.

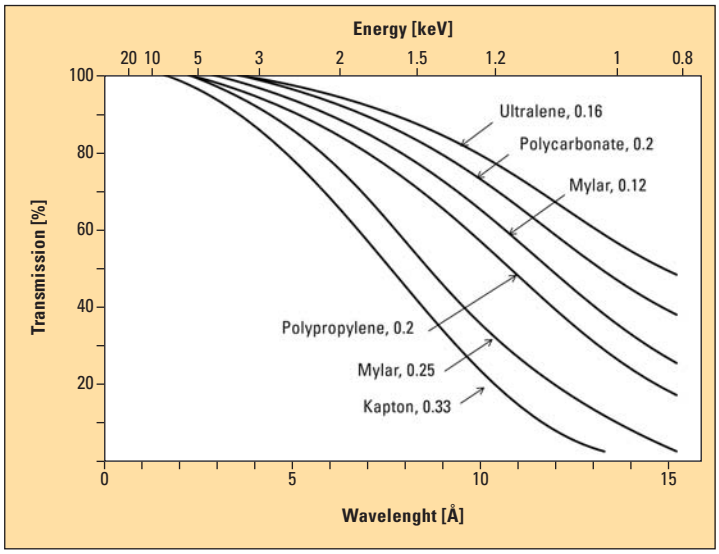

Figure 2: Transmission capacity of various polymer films as a function of the wavelength of the incident X-ray radiation. Lighter elements exhibit a higher wavelength and a lower energy. They are found at the right-hand side of the graphic.

Burning high-tech

Graphite tubes for electrothermal atomization

Figure 1: AA-7000 atomic absorption spectrometer with GFA-7000 graphite furnace atomizer

In graphite furnace technology, it is important to select the graphite tube according to the target element and sample composition. In fact, a wide variety of graphite tubes are used in electrothermal atomization. The AA-7000 atomic absorption spectrometer in combination with the high-sensitivity digitally controlled GFA-7000 graphite furnace atomizer can be operated with the following tube types: high-density graphite tube, pyrolytic-coated graphite tube, "fork"-platform graphite tube and omega platform tube®.

Made of ordinary graphite, the high-density tube is widely used. Since the hexagonal graphite crystal structure has porous characteristics, the injected sample solution permeates into the graphite tube wall during the heating process. On the other hand, the pyrolytic-coating tube has a metallic shining surface, made by formation of a pyrolytic layer through chemical vapor deposition. Since the density of the surface is higher than that of a high density tube, sample permeation into the wall is lower and the generation of the atomic cloud during the atomization stage is improved. The platform tube refers to a graphite tube in which a plate with a basin for the sample (platform) is mounted. The Shimadzu platform tube has a platform made of 100 % pyrolytic carbon. Figure 2 shows a comparison of peak profiles of pyrolytic-coated tube and the high-density tube.

High-density tube specializes in elements with low atomization temperatures

The high-density tube is used for measurements of various elements, especially for those showing low atomization temperatures, such as cadmium (Cd), lead (Pb), sodium (Na), potassium (K), zinc (Zn) and magnesium (Mg). It is also useful to reduce the measurement sensitivity of an element in case of high concentration samples.

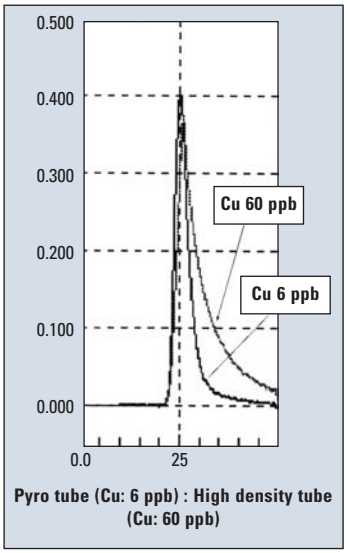

Figure 2: Comparison of peak profiles of pyrolytic-coated (6 ppb) and high density tube (60 ppb)

For example, in case of aluminum, iron and copper, although a level of 1 ppb can be measured using the pyrolytic-coated tube, the sensitivity can be reduced by a factor of 100 to a level of 100 ppb using the high-density tube.

Figure 3 shows an example of calibration curves for Cu measurements using the high-density tube and the pyrolytic-coated tube. The measurement points are 20, 40 and 60 ppb in the case of high-density tube and 2, 4 and 6 ppb in the case of pyrolytic-coated tube, although similar absorbance values are shown.

Pyrolytic-coated tube shows sharp peaks for carbide-forming elements

In general, the pyrolytic-coated graphite tube is the most effective solution for elements which easily form carbides as a reaction with the graphite in an uncoated tube. Nickel (Ni), calcium (Ca), titanium (Ti), silicon (Si), vanadium (V) and molybdenum (Mo) are elements typically showing this effect. In the high-density tube, a sample easily permeates into the graphite, resulting in a larger contact area between the element and carbon. In the pyrolytic-coated tube, however, a smaller contact area can suppress carbide formation, and a higher sensitivity is obtained as a result. When the peak profiles are compared, a sharp peak is observed in the case of pyrolytic-coated tube, while a broad peak is observed in the case of high-density tube. Figure 2 shows the example for copper.

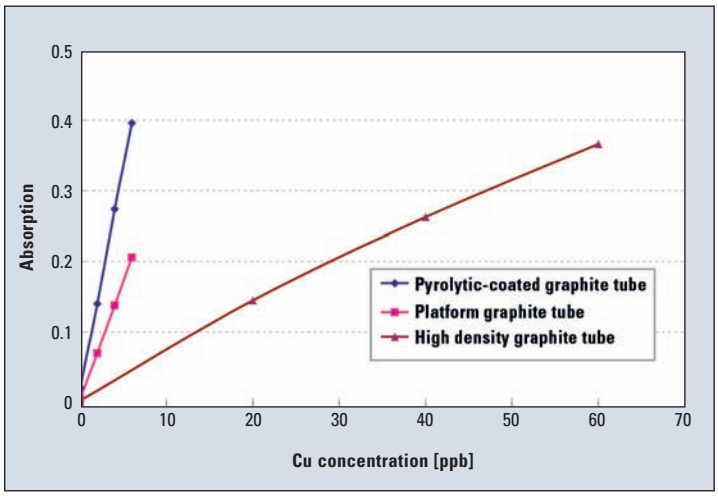

Figure 3: Sensitivity comparison of graphite tube types

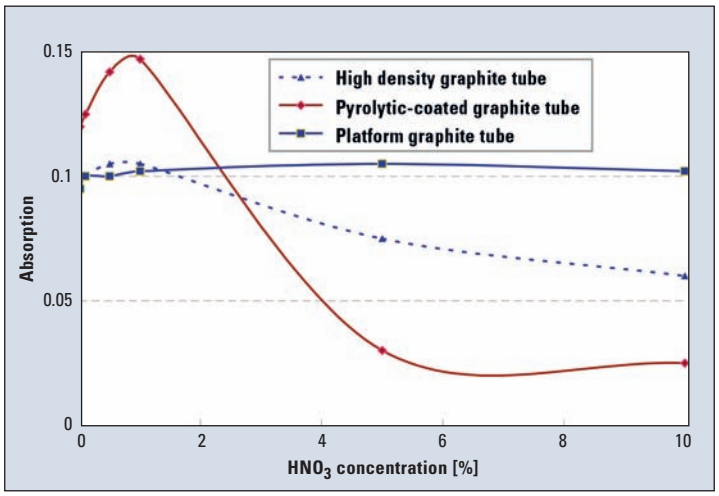

Figure 4: Effect of nitric acid concentration on Pb sensitivity among graphite tube types (Pb: 5 ppb, 10 µL injection)

Acid concentration affects sensitivity and reproducibility

Furthermore, variation of the acid concentration has a significant effect on the sensitivity and reproducibility of the analytical result. The effect of nitric acid concentration on the sensitivity of lead is shown in figure 4. When comparing different graphite tubes, the sensitivity varies more drastically as the acid concentration changes. In the case of a pyrolytic-coated tube, however, the analytical result is easily affected by the acid concentration in the sample. Compared to platform or high-density tubes, the sensitivity varies more drastically as the acid concentration changes.

As a feature of the platform tube (Figure 5), the sample solution is injected onto the platform and has no direct contact with the wall of the graphite tube. It is then heated according to the element-specific heating program.

During electrothermal atomization, the graphite tube is heated firstly by the wall. Therefore, in a standard graphite tube such as the high-density or the pyrolytic-coated tube, the sample is heated and atomized as the wall is heated. In a platform tube, however, the sample is atomized after the temperature of the entire tube reaches the atomization temperature, so the sample is atomized under optimum temperature distribution. When measuring with platform tube, the atomization peak becomes broader although the platform material is pyrolytic graphite (Figure 6).

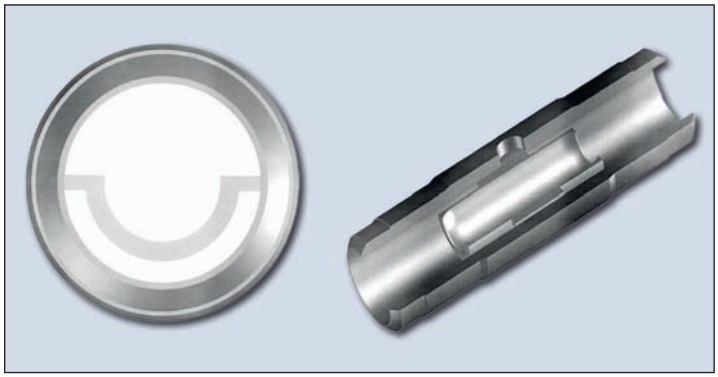

Figure 5: Omega platform tube®

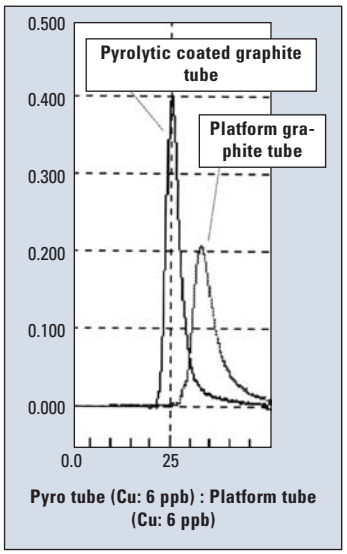

Figure 6: Comparison of peak profiles of pyrolytic-coated (6 ppb) and platform graphite tube (60 ppb)

Platform tube is the effective solution for complex matrix samples

The platform tube requires the temperature for ashing and atomization to be set at a value of 100 °C to 200 °C higher than normal pyrolytic-coated tubes. The difference in the heating characteristics of the platform tube in comparison to a standard tube minimizes the influence of matrix effects of complex samples, so the background signal is separated clearly from the element signal, especially in combination with matrix modifiers such as palladium, iridium, rhodium and others. Use of the platform tube and matrix modification is therefore the most effective solution for the determination of elements in samples with complex matrix, such as biological sample, waste water and seawater.

Replacement liver for sim

Figure 1: Surgical instruments used in keyhole surgery ('minimal invasive surgery')

Sylvia Donner, Marc Kraft
TU Berlin, Germany
ZMMS, GRK prometei/
FG Medizintechnik

In medicine and medical technology, animal tissues – in most cases pig tissue – are often used for testing products or devices that are intended for use on humans. Like all natural materials, animal tissue is also subject to strong fluctuations, and (mechanical) material parameters vary strongly. Reproducible experimental conditions can therefore only be guaranteed to a limited extent. Storage conditions, age of the sample and the particularity of the animal are some of the most important factors influencing the properties of animal materials.

In order to simulate a so-called keyhole surgical procedure – a laparoscopic gall bladder removal – a replacement tissue for the liver had to be found. In this intervention, the gall bladder positioned under the liver is removed via three to four small skin cuttings in the abdominal wall. In contrast to conventional procedures, the abdominal wall remains virtually closed.

An advantage for patients, a challenge for surgeons

Patients benefit greatly from this procedure – compared to open surgical procedures the pain experienced is significantly less, and leads to a better cosmetic result due to reduced scarring.

On the other hand, the freedom of movement and vision for the surgeon is severely limited. Surgery is only possible by using specialized instruments (Fig. 1). Performing surgery under these conditions presents physical challenges for the surgeon, some of which can be attributed directly to the instruments used [2]. This is why guidelines for the design of laparoscopic (gripping) instruments are currently being developed to take into account not only the safety of the patient but also the ergonomic aspects for the surgeon. However, for ethical reasons measurements during real surgical procedures are not feasible at all or only with considerable restrictions.

The liver is in the way

During a gall bladder removal, the liver plays an important role, especially due to the anatomical proximity of both organs. During surgery or simulation, the liver must be held to the side for a relatively long time to obtain access to the gall bladder, which is why a uniform replacement material is required that is equipped with similar gripping properties. For this purpose, tensile strength tests were carried out on pig liver samples in order to determine the mechanical material parameters of an average pig liver.

So far, relatively little research has been carried out on material parameters of animal tissues. The techniques described in a standard work by Yamada [5] are no longer state-of-the-art. For instance, Yamada describes tensile tests using suspended weights on a relatively small number of samples. The tensile properties were based on tensile tests carried out in 1953 on several rabbit livers. Due to the methodology they were presented in g/mm^2. In more recent research, these classical tensile tests were abandoned in favor of other methods. Mazza, for instance, used compression tests on the liver of living patients to determine the material parameters in 2008 [3].

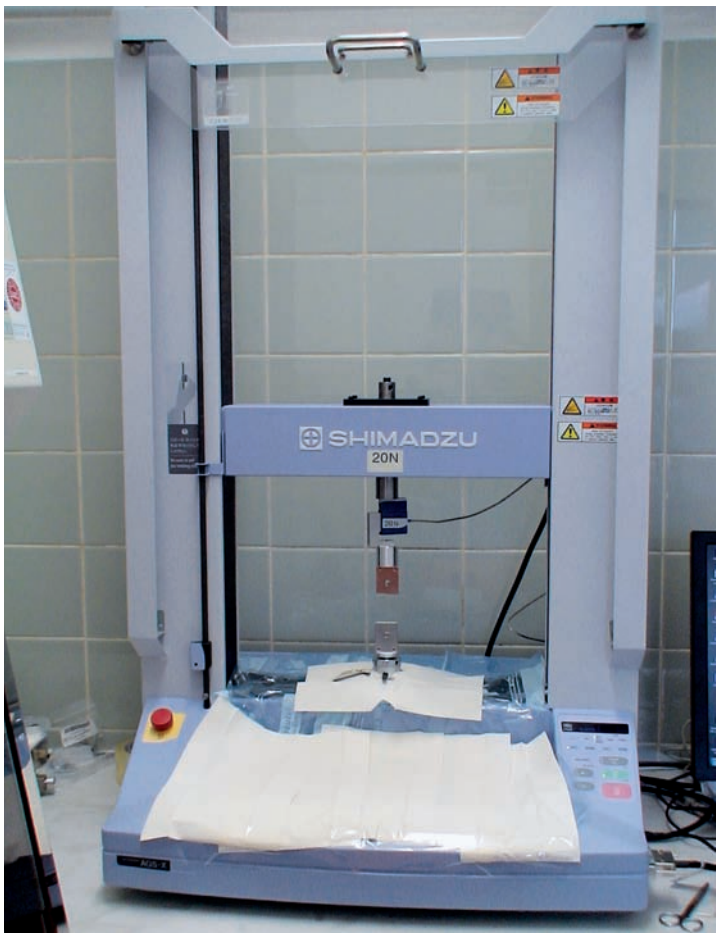

Figure 2: Shimadzu's AGS-X universal testing machine specially prepared for the experiments and used in the tensile tests

ulation of keyhole surgery

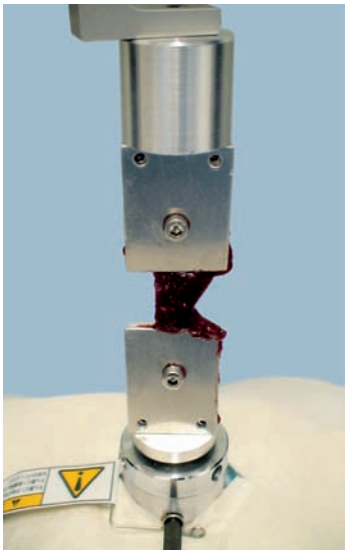

Figure 3: Clamped pig liver sample

How to find 'replacement livers'

In order to determine the material parameters, experiments had to be carried out. Due to the lack of test specifications, own test routines had to be developed. These were built upon existing standards, such as DIN EN ISO 527 for the determination of tensile properties of plastics [1]. The tensile tests were carried out at room temperature (approximately 20 °C), on a 20 N Shimadzu AGS-X universal testing machine (Figure 2).

Clamping a total of 52 standardized pig liver samples with portions of exterior tissue presented a challenge. Due to the particular consistency of the animal tissue, existing clamping devices could not be used. The spring grips used next destroyed the samples because the local pressure load was too high. This is why own clamping devices have been designed to clamp all samples (Figure 3). The samples were stretched with the AGS-X universal testing machine at a rate of one Newton per minute until rupture. Own MATLAB® algorithms (The MathWorks) have been used to analyze the raw data.

As expected, the stress-strain curves obtained exhibited strong scattering. For the evaluation, it was therefore necessary to firstly define rogue results for which the maximum stress lies outside the range between the lower and upper quarter of the samples.

Of the remaining data sets, mean values were established and a best-fit curve, a polynomial of the 9th order, was approximated. The curve had a linear range and the elastic modulus could therefore be determined as $6.28*10^{-2}$ N.mm^2 (62.8 kPa) at an elongation of 54 % (Figure 4). Using these values, it was possible to find a replacement material – a PUR-ether foam – possessing similar mechanical tensile properties.

The 'replacement liver' found this way is currently used in surgical simulations (Figure 5) as well as for the continued study of laparoscopic gripping devices. The replacement material therefore also serves in additional studies to formulate a defined load for the medical instrument industry. In this way, it is possible to investigate locking mechanisms that enable tissues to be clamped over longer periods of time without excessive strain. The target is to develop a gripping mechanism that will, on the one hand, meet ergonomic requirements for the protection of the doctor as well as being easy to apply and to release. On the other hand, a longer clamping duration shall not lead to any damage of the patient's tissues.

In contrast to the use of animal material, all studies on the use of synthetic materials are reproducible. In addition, the results can be compared with each other. Realistic replacement materials therefore offer an important foundation for all relevant studies.

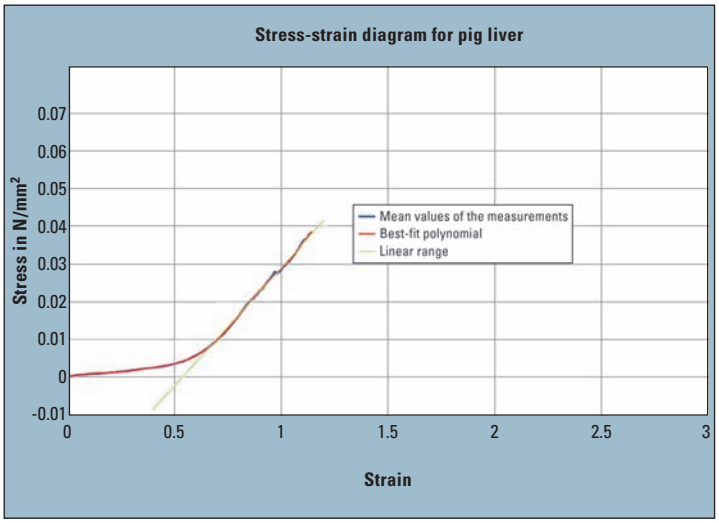

Figure 4: Stress-strain diagram for pig liver: representation of the mean values of the measurements without outliers (blue), the best-fit polynomial (red) as well as the linear range (green)

Figure 5: Simulation of a laparoscopic gall bladder removal using artificial materials

Literature

[1] DIN EN ISO 527-1: 2010 Kunststoffe – Bestimmung der Zugeigenschaften / Plastics – Determination of tensile properties

[2] Donner, S.; Kraft, M. (2010): Potentiale zur verbesserten Gestaltung von minimalinvasiven Chirurgieinstrumenten – Auswertung einer Befragung unter laparoskopisch operierenden Chirurgen. In: Grundlagen – Methoden – Technologien / 5. VDI Fachtagung Useware 2010. Baden-Baden, 13. und 14. Oktober 2010. Düsseldorf: VDI-Verlag, S. 179-188

[3] Mazza, E.; Grau, P.; Hollenstein, M.; Bajka, M. (2008): Constitutive Modeling of Human Liver Based on in Vivo. MICCAI 2008, Part II, LNCS 5242, 2008: 726-733

[4] Ohara, T (1953): On the comparison of strengths of the various organ-tissues. J. Kyoto Pref. Med. Univ., 53: 577-597

[5] Yamada, H (1970). Strength of Biological Materials. The Williams & Wilkins Company, Baltimore, 1970

Soft materials in hard drinks

Occurrence of endocrine disruptors in foods

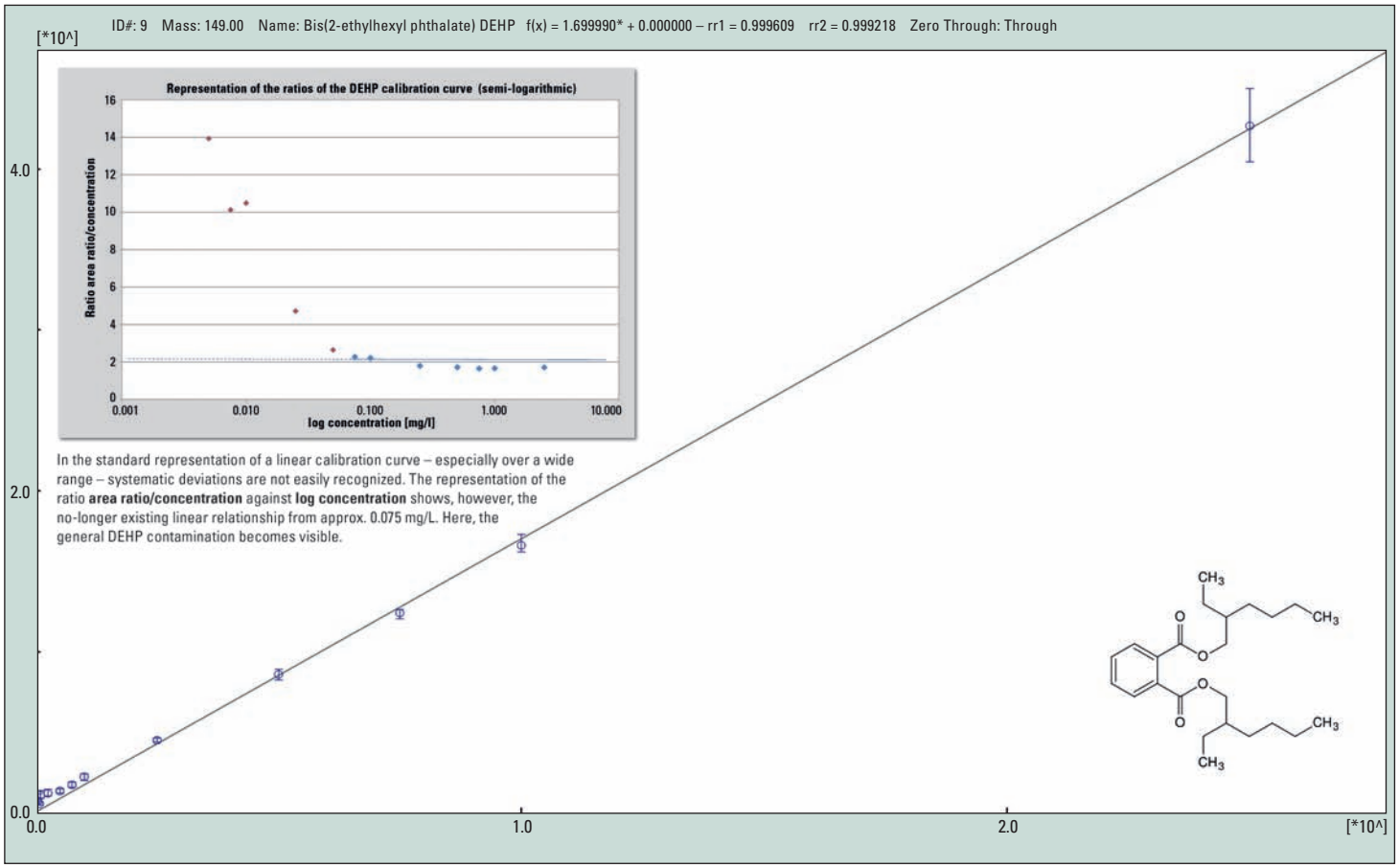

Figure 1: Calibration of DEPH (diethylhexyl phthalate) within the range of 5 pg/µL - 2500 pg/µL

Plastics such as polyethylene, polypropylene and polyvinyl chloride are long-chain polymers. In addition to the chemical composition of the polymer, its desired properties also depend on the admixture of additives. The most widely used additives are plasticizers such as phthalates, bisphenol A and nonylphenol.

This group of plasticizers contains substances with hormone-like properties. These endocrine disruptors are considered as critical due to their ability to migrate and their toxic potential. It is therefore important to keep any contamination with endocrine disruptors as low as possible for risk groups such as infants, children, adolescents and pregnant women (ALARA principle*). An overview of the tolerable intake levels of the main phthalate DEHP – diethylhexyl phthalate – is presented in table 2.

Plasticizers are everywhere

The phthalic acid esters (phthalates) mainly used as plasticizers are found in paints, varnishes, adhesives, plastics, gaskets, cosmetics, toys, packaging and in medicinal products – to mention just a few. Due to the large-scale use of phthalates in all types of plastics, many of these compounds are ubiquitous. In house dust they have been detected repeatedly [1, 2].

To detect an increased phthalate contamination, its concentration is determined using analytical instrumentation. For many application areas, appropriate testing procedures have been described and are required by law (e.g. EPA 506 (5), DIN EN ISO 18856:2005 for water analysis).

For instance, PVC (foils, flooring) often contains 20 % to 30 % plasticizers. They can be considered as main components. Analysis using FTIR-ATR and GC/MS is easy. The ubiquitous occurrence (such as DEHP) hardly affects the result, as a contamination is only expected in trace-amounts and this is, in the double-digit percentage range, negligible.

Phthalates detectable even in PET beverage bottles

Other plastics, such as PET (polyethylene terephthalate) should not contain any phthalates. Due to improper recycling, however, thermal stress or migration from the imprint, phthalate contamination cannot be excluded. These are mainly trace-amounts that may be released into beverages such as mineral water or juices. After consumption they can be incorporated into the body. Table 1 shows the analysis results of a study on a commercial cola flavor soft drink. Several phthalates could be detected in trace amounts. The analytical determination was car-

ID#	Analysis	Result	Unit	Method
1	Dimethyl phthalate (DMP)	0.65	µg/L	GC-MS
2	Diethyl phthalate (DEP)	1.07	µg/L	GC-MS
4	Nonylphenol (NP)	0.97	µg/L	GC-MS
5	Di-n-butyl phthalate DBP	1.55	µg/L	GC-MS
6	Bisphenol A	N.D.	µg/L	GC-MS
7	Bis(2-ethylhexyl) adipate DEHA	1.28	µg/L	GC-MS
8	Benzyl butyl phthalate BBP	0.25	µg/L	GC-MS
9	Bis(2-ethylhexyl) phthalate DEHP	1.87	µg/L	GC-MS
10	Di-n-octyl phthalate DNOP	0.46	µg/L	GC-MS

Table 1: Content of phthalates, bisphenol A and nonylphenol in a cola-flavored soft drink in a polyethylene (LD-PE) bottle (excerpt from analysis report)

ried out using GC/MS after sample preparation. The small amount of analyte requires a high sensitivity of the instrumental system. The combination of Shimadzu's GC-2010 Plus with the QP-2010 Ultra MSD easily meets this requirement.

Figure 1 shows the ubiquitous presence of the phthalate DEHP using a calibration curve. The linear range of the detection method is limited by the carry-over of trace components in the lower concentration range, despite the use of high-purity grade laboratory chemicals. Special precautions during sample preparation as well as in the selection of materials and laboratory chemicals are therefore needed to prevent erroneous measurements as much as possible.

In the usual representation of a linear calibration curve – particularly over a wide range – systematic deviations are hardly recognizable. In contrast, the representation of the ratio area ratio/concentration against log concentration in figure 1 shows that a linear relationship is no longer present from approximately

Chromatographic conditions:
Shimadzu GC QP-2010 Plus with MSD QP-2010 Ultra, column Macherey & Nagel Optima delta-3 - 0.10 µm 10 m x 0.1 mm ID, split 1:25, purge 3 mL/min, linear velocity 30 cm/s, temperature program 130 °C - 0.2 min, 40 °C/min to 270 °C, 60 °C/min to 320 °C - 3.0 min

0.075 mg/L. Here, the overall DEHP contamination becomes evident. The detectable unilateral deviations from the horizontal that can be determined in the lower concentration range are caused by the "blank content."

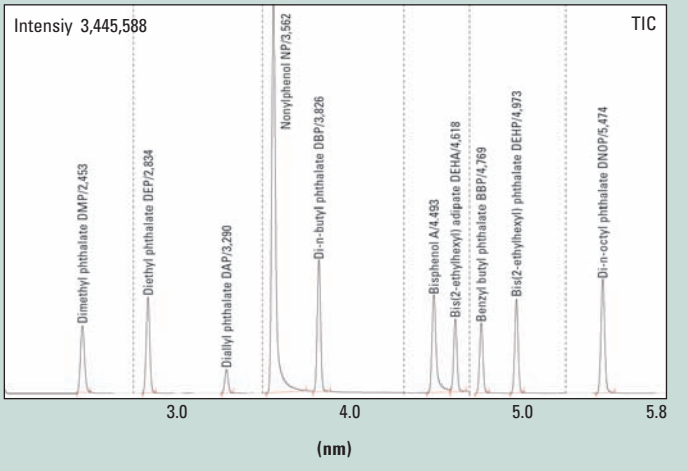

Figure 2: Example of a SIM chromatogram of a phthalate mixture, approx 2.5 ng/µL; Conditions: split ratio 1:25, septum Supelco Thermogreen LB2, column Macharey & Nagel Optima delta 3; 10 m x 0.1 mm ID x 0.1 µm film thickness

Institution	TDI's	Value (µg/kg KG/d)	Year
NL-RIVM	TDIa	4	2002
US-EPA	RfDc	20	1991
WHO	TDIa	25	2003
EU-CSTEE	TDIa	37	1998
ECB/EU	TDIa	20 (Infants 0 - 3 months and women of childbearing age)	2004
		25 (Infants > 3 - 12 months)	
		48 (Rest of the general population)	
D-UBA	TRDd	50	2003
BfR and EFSA	TDIa	50	2005
	a: Tolerable daily intake b: Maximum permissible risk level c: Reference dose (for chronic exposure) d: Tolerable resorbed dose e: Minimal risk level (for chronic exposure duration)		

Table 2: Overview of tolerable intake levels of DEHP[6]

Strategies for the prevention of phthalate contamination

In principle, the determination of phthalates in trace quantities requires the use of phthalate-free instruments and materials – usually glass and aluminum [3]. These materials can be cleaned easily using thermal decontamination [4].

Suitable methods have been described in the DIN EN ISO 18856:2005 standard. Solvents must be tested prior to use to determine if they are free from phthalates. Septa and liners must meet these requirements as well. Additional measures such as silanization (hexamethyldisilazane) also help in reducing the measurement uncertainty. By using fast GC, multiple determinations can be realized within short analysis times (see Fig. 3).

Endocrine disruptors
Endocrine disruptors occupy specific receptors, replace hormones and upset the hormone balance in the human body. This can lead to impairment of growth, development and reproductive processes. Examples are developmental disorders, birth defects, premature puberty in girls, reproductive problems as well as a decrease in sperm count.

References

[1] Fromme, H., et al., et al. Occurence of phthalates and musk fragrances in indoor air and dust from appartments and kindergartens in Berlin (Germany). Indoor Air, 2004, 14, 188-195
[2] Scharf, S., Uhl, M. and Hohenblum, P. Hausstaub – Ein Indikator für Innenraumbelastung. Umweltbundesamt Österreich, Wien, 2004, 258
[3] Brüll, U., Alberti, J. and Furtmann, K. Phthalatanalytik in Wasser und Sediment. Landesumweltamt NRW, 45023 Essen
[4] Saido, Katsuhiko, et al., et al. Thermal Stability of Phthalic Esters. Journal of the American Oil Chemists' Society, 1984, (61[5]), 945-949

Glass on the road increases driv

Particle measurement of glass beads

"To see and be seen" in road traffic means more safety for all. At night, reflectors improve the visibility of non-self illuminating objects and road users. Roughly three types of reflection occur: diffuse reflection, mirror reflection and retroreflection.

In diffuse reflection, the main backscatter takes place perpendicular to the material, independent of the incident direction of the radiation. Examples are milk, wall paints or paper. In mirror reflection, the reflected light retains its parallelism. The angle of incidence is the same as the angle of reflection.

In the case of retroreflection, as much as possible of the light emitted from the source is reflected back to its origin. Light from a car headlight, for example, is reflected toward the driver's eye. The principle of retroreflection is applied successfully in traffic signs and pavement markings.

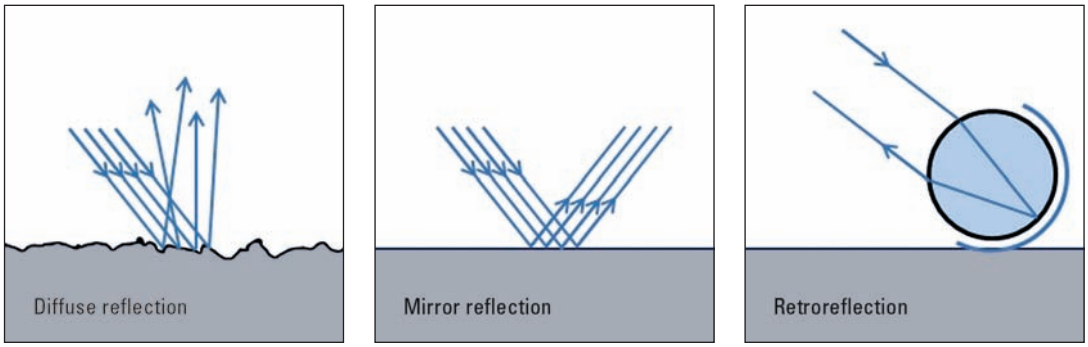

Figure 1: Diffuse, mirror and retroreflection

Glass beads in retroreflective materials

One possibility for the manufacture of retroreflective materials is the embedding of small glass beads within the surface of the material. In addition, the back surface of these beads can be coated with a reflecting layer. As soon as light hits the beads, the incident light is reflected back in its original direction due to the dual refraction within the bead.

Pavement markings often seem to be visible to varying degrees under wet road conditions in the dark. Indeed, there are two different types of markings.

Marking techniques in the past used glass beads and antiskid materials that were scattered onto the thinly applied and still wet paint to attain the desired visibility, also at night.

There are, however, problems with these types of pavement markings under wet road condi-

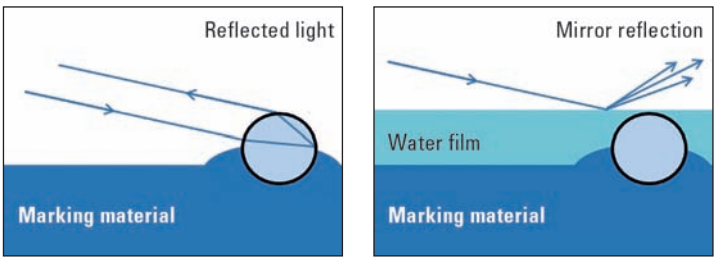

Figure 2: Performance of different marking types on a dry or wet road

ing safety

tions, when a thin film of water covers the road as well as the markings. The water film reduces retroreflection and decreases visibility of the markings at night considerably in wet conditions.

Literally outstanding – a new marking method

For these reasons a new marking method has been developed that ensures good visibility, also at night and under wet conditions. This method has, therefore, largely replaced all conventional methods.

Virtually all markings of the older type have meanwhile been replaced on German highways.

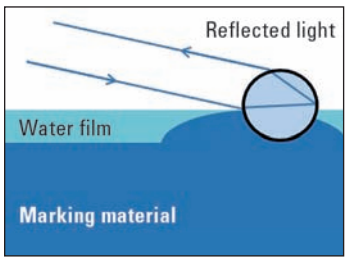

Markings of the newer type have been applied on approximately 70 % of all German roads. They protrude from the water film on the road by several millimeters, ensuring that retroreflection continues to occur within the glass beads.

Particle measurement of the glass beads

The beads typically exhibit a diameter of approx. 50 µm. In order to verify the size distribution of the beads, particle measurement was carried out using Shimadzu's SALD-7101.

The glass beads were suspended in water using several drops of a tenside. In order to prevent the beads from sinking to the bottom of the measuring cell (BC-71), they were kept in motion using a stirrer.

As can be seen from the spectrum and as expected, a size distribution of the beads around 50 µm could be measured. Using the SALD-7101 system including the BC-71, it was possible to reliably measure the size distribution of glass beads.

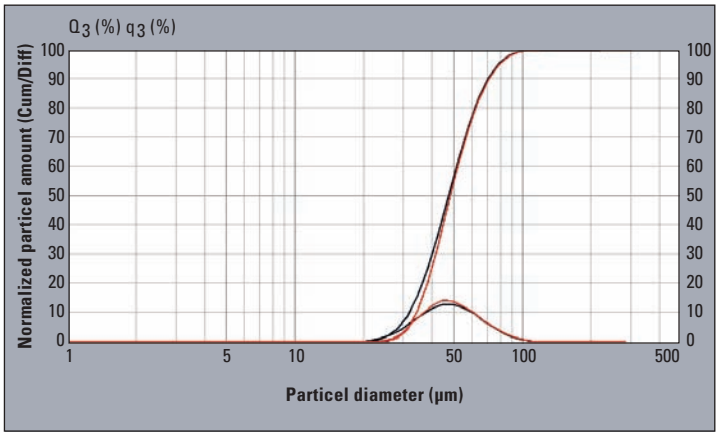

#	Color	Median D [µm]	Modal D [µm]	Mean D [µm]	Std. dev.	Ref. Index
1	black	47.146	44.668	47.245	0.134	1.80 - 0.00i
2	red	47.957	44.668	48.718	0.123	2.00 - 0.00i

Figure 3: Size distribution of the glass beads

Almost omnipresent

Determination of bisphenol A in plastic packaging

Troisi Jacopo, Di Fiore Raffaele
Laboratorio Chimico Merceologico, Az. Spec.
CCIAA Napoli, Italy
Palumbo Giancarlo
Università Federico II, Dottorando di Ricerca in "Scienza dell'Alimentazione e della Nutrizione", XXV ciclo, coordinatore: Prof. Franco Contaldo, Tutor: Prof. Maria Valletrisco

Bisphenol A (BPA) is mainly used in the production of plastics; its by-products have been commercially available for over 50 years. BPA is also applied in the synthesis of polyesters, polysulfonates, as antioxidant in some plasticizers and as inhibitor against PVC polymerization.

Above all, however, BPA is the key monomer in the production of epoxy resins and the majority of polycarbonates. Polycarbonates are transparent and virtually unbreakable and are therefore found in numerous childrens products as well as in bottles, sports goods, health care, dental and optical equipment, in spectacle lenses, household equipment and in protective helmets – wherever durable or long-lasting materials are needed. On the other hand, BPA-containing epoxy resins are used as internal coatings in many steel cans for foods and beverages. BPA is also a precursor of flame-retardants and has been used in the past as a fungicide.

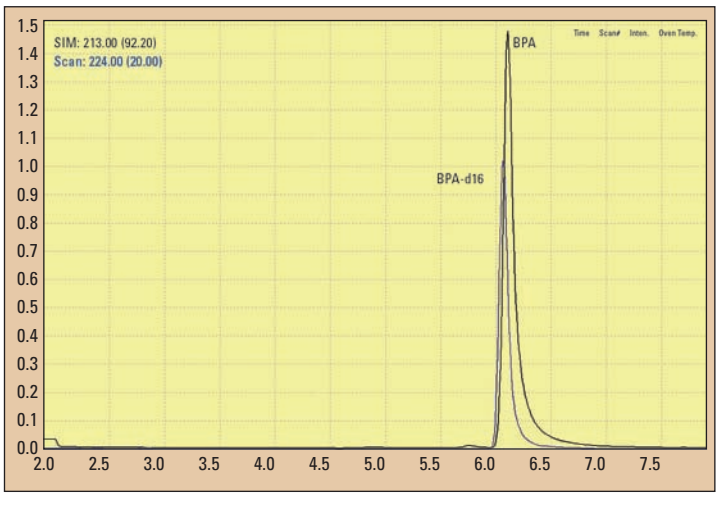

Figure 1: Gas chromatogram (TIC) of a BPA and BPA-d16 standard

Suspected since the 1930's to be harmful to humans, concerns regarding the use of BPA-containing plastic materials have increased considerably in 2008, as many governments commissioned studies on the safety of BPA. Some distributors have withdrawn products containing BPA from the market. BPA seems to be mainly responsible for numerous impairments in male and female sexual development during the fetal stage, as well as a decline in fertility during adulthood.

BPA and hormonal activity

Worldwide production of BPA was estimated at two million tons

in 2010. BPA alters the activity of the endocrine system by activating hormone receptors. In case of elevated doses, this can have negative consequences for health. Experimental studies have shown that BPA mimics the activity of estrogen (essential for brain development) to such an extent that even the smallest doses can completely inhibit the activity of estrogen and its effects on neuronal growth. Although BPA-based polymeric packaging materials are considered to be stable under normal circumstances, they can still release small but toxicologically significant amounts of BPA so that an increased risk exists that beverages or foods are contaminated with this substance.

BPA has also been associated with the development of numerous other clinical conditions of the reproductive organs, the prostate and the female breast. The studies conducted, show clear evidence of endocrine effects and make it possible to define a daily maximum recommended dose of 0.05 mg/kg body weight [1].

Long-term risks cannot be ruled out

In September 2008, the US National Institute of Environmental Health Sciences issued a brief for the assessment of human health risks that is based on the result of the complex points of contact between food, consumer products and living conditions [2]. The document compared the effects of BPA in experimental studies and the associated 'dosage-response' data with existing information on the level of risks of human exposure to the compound, including the limited epidemiological studies and biological monitoring carried out to date.

The conclusions rule out any risk to reproductive health and pregnancy in adults. Nevertheless, the concerns on long-term risks to the endocrine, neurological and reproductive development as a result of exposure in utero and/or during childhood remain.

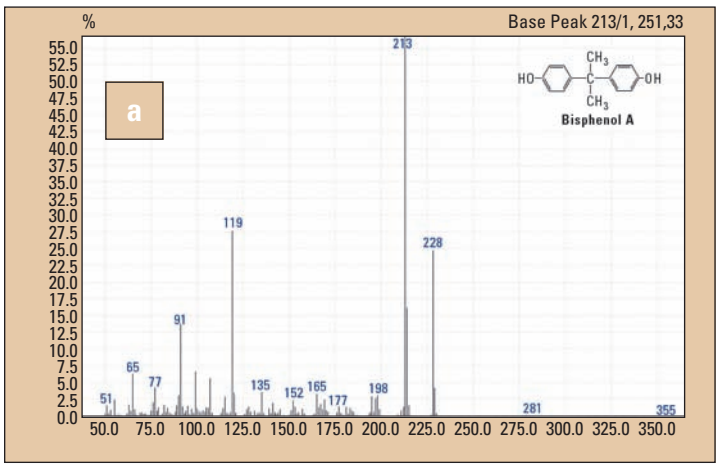

Figure 2: Mass spectra of BPA (a) and BPA-d16 (b)

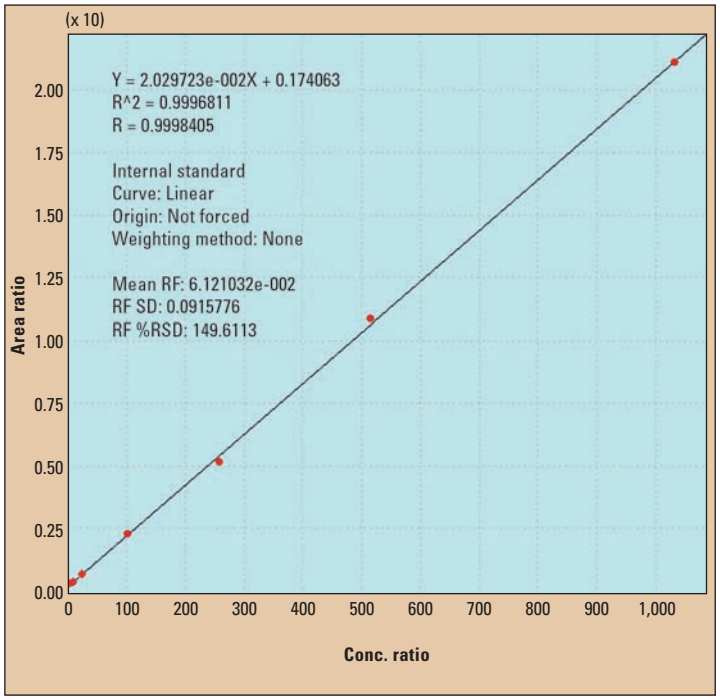

Figure 3: GCMS calibration curve of BPA

As of 28 January 2011, Europe has banned BPA-containing baby bottles according to the European Union directive 2011/8/UE. Since 1 March 2011, the manufacture of BPA-containing baby bottles has been prohibited and from 1 June 2011, this ban also applies to sale and import.

Research group polycarbonate/BPA

The American Chemistry Council, Plastics Europe and the Japan Chemical Industry Association have joined forces to form a polycarbonate/BPA research group (www.bisphenol-A.org). This group has also defined the determination of BPA under different conditions (environment, biological and plastic materials) [3]. According to these criteria, gas chromatography coupled to mass spectrometry (GC-MS) is the method of choice for the determination of BPA, whereby confirmation is based on the ratio of the signals at 228 m/z and 213 m/z. Nevertheless, a large part of scientific work published to date has reported the use of HPLC-MS-MS methods for the determination of BPA. This discrepancy may be due to the need to detect even the smallest amounts, which has been difficult to achieve with the GC-MS systems.

Materials and methods

Two methods for the determination of BPA are presented: a GC-MS method using a GC-MS-QP2010 system and an LC-MS method using the single Quad LCMS-2010 system. In both cases the detection limit is approximately 0.1 µg/L.

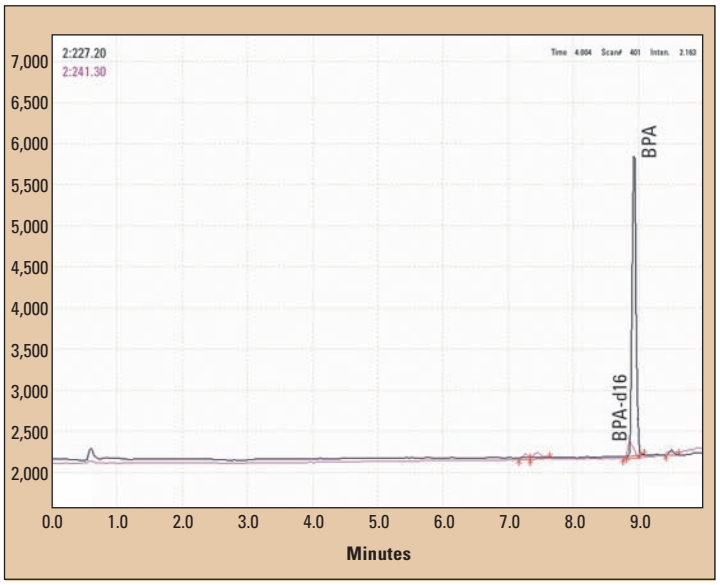

Figure 4: LCMS chromatogram of a BPA and BPA-d16 standard

BPA determination using GC-MS

The GC-MS method is based on a Supelco® SLB®-5ms column with a length of 15 m and an internal diameter of 0.1 mm with a film thickness of 0.1 µm. The GC oven program includes an initial phase of 1.5 minutes to 160 °C and two heating rates: first 20 °C/min up to 260 °C, then 40 °C/min to 320 °C. The injection temperature is 260 °C and the linear carrier gas velocity (helium) is 50 cm/sec. This setting requires a pressure of more than 700 kPa and a linear flow of 0.86 mL/min. The total cycle time is 8 min; the maximum retention time is 5.9 min.

These fast analysis times require high data acquisition rates. Two data acquisition channels were used, one in the SIM mode and the other in the SCAN mode between m/z = 50 and m/z = 500. The so-called 'event time' for the SCAN mode was set to 0.1 sec (corresponding to a scan rate of 5000 amu/sec, half of the maximum rate attainable using the QP-2010). In the SIM mode, the ions m/z = 213 and m/z = 228 for BPA and m/z = 224 for the internal standard were measured.

Calibration was carried out using eight standard solutions at a concentration of 0.1 µg/L up to 1,000 µg/L. This method has been proven to be extremely reliable.

Argus eyes

New class of UV-VIS double-beam spectrophotometers

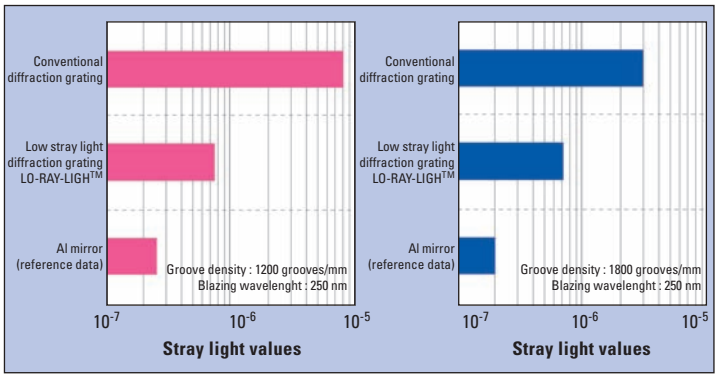

Figure 1: Representation of stray light and comparison between a conventional grating, a LO-RAY-LIGH grating and an aluminum reference

Shimadzu's role as world-wide market leader in UV-VIS double-beam spectrophotometers means continuous challenges for R&D to meet the high expectations of users from all over the world and to set standards in instrument development. Shimadzu designs not only complete analytical systems but also the optical components for a spectrophotometer. This article focuses on a patented development in diffraction grating technology.

New holographic exposure method

Shimadzu has optimized the quality of the edges for the angle of reflection in the sawtooth pattern using a new holographic exposure method. This LO-RAY-LIGH® principle is a patented development that produces an outstanding grating quality. Until now, the generally accepted rule was: the more lines to a grating, the sharper the spectral image. With the LO-RAY-LIGH® grating technology, this has changed. The production process of the grating results in a high grating image precision which also yields a spectral resolution sharpness rendering better characteristics when compared to a conventional grating.

The objective in the development of these gratings was a significant reduction in stray light.

Sharper image

Figure 1 shows the stray light values for a conventional grating and the LO-RAY-LIGH grating. In the logarithmic scale it is apparent that the LO-RAY-LIGH grating enables an exceptionally high reduction of stray light.

For the qualification of a grating, the intensity of the first-order light is plotted against delta (nm). From figure 2 it becomes evident that the LO-RAY-LIGH grating produces first-order light much more sharply and with less stray light over the entire range. In the diagram, a grating of groove density 1,200 grooves/mm was compared with a blaze wavelength of 250 nm.

New optics improve quality

The quality of the optical components becomes noticeable during the measurements. Shimadzu's UV-2700 spectrophotometer is equipped with double monochromator optics containing two of these new gratings. The effect is significant. An example is the linearity measurement of a $KMnO_4$ dilution series where the difference to Shimadzu's previous UV-2550 model from the same class becomes evident. While the UV-2550 already exhibits a strong noise at six absorption units, the new UV-2700 UV-VIS spectrophotometer features exceptional linear characteristics up to eight absorption units.

With respect to the number of grid lines, the UV-2550 exhibits 1,600 lines/mm and the new

Measurement was performed using an internal deuterated standard (BPA-d16).

Determination of BPA using HPLC-MS

The HPLC-MS method, on the other hand, is based on a 50 mm x 2 mm Shim-Pack XR-ODS column. Chromatographic separation is carried out using a water/methanol gradient. The gradient program includes an initial phase of one minute using 20 % methanol with an increase up to 50 % within 5 minutes, then an additional ramp up to 100 % in a further five minutes, followed by a return to the initial conditions (20 % methanol) in a further two minutes, and finally an equilibration of three minutes. The total analysis time is 15 minutes. The flow rate is 0.2 mL/min.

Also in this case, data acquisition was carried out in the SCAN mode (measuring negative ions) between m/z = 180 and m/z = 480 as well as in the SIM mode (negative ions) m/z = 227.20 and m/z = 242.30. The ion source was adjusted to - 3.5 kV, the desolvation line to 250 °C. Flow rate of the nebulizer gas was 1.5 L/min.

Conclusions

The possibility to quantify BPA with increased sensitivity in both GCMS and LCMS is an essential requirement for the analysis of samples from different origins. Since the first investigations have been carried out, BPA appears to be widely present in many everyday objects – even though in low concentrations. Only through efficient quantification of BPA present in various sources will it be possible to assess the actual level of risk to humans and the effect of BPA as an endocrine disruptor.

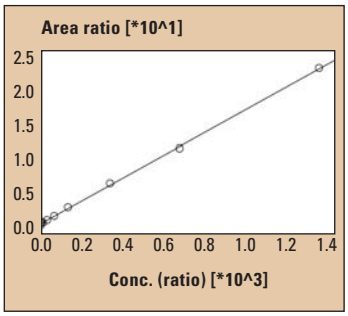

Figure 5: LCMS calibration curve of BPA

References

[1] EFSA panel on food additives, flavourings, processing aids and materials in contact with foods – Efsa Journal Jan 2007doi: 10.2903/jefsa.2007.428

[2] NTP-CERHR monograph on the potentional human reproductive and developmental effect of Bisphenol A – NIH Publication No.08-5994 Set 2008

[3] www.bisphenol-a.org/pdf/criteria_102002.pdf

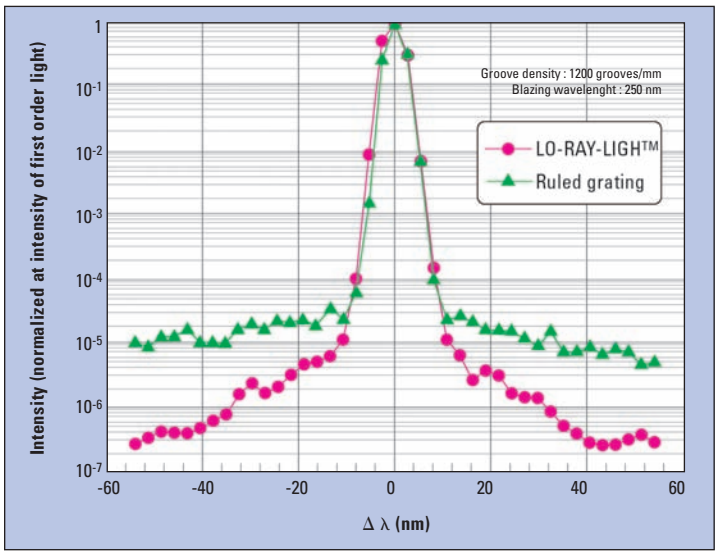

Figure 2: Representation of the intensity of the first-order light as a function of the distance to the origin of the wavelengths in nm

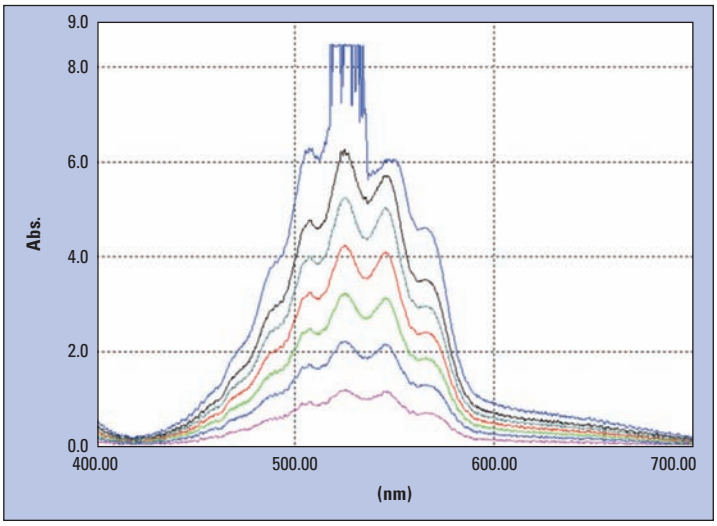

Figure 4: UV-VIS spectra of a potassium permanganate dilution series of 6 to 1 absorption units measured using the UV-2550 equipped with conventional gratings

UV-2700 instrument exhibits 1,300 lines/mm. This reduced grid line number results in better measurement characteristics for the new grating compared with the conventional grating featuring a higher grid line number.

With this objective in mind when developing the instrument, the UV-2700 is recommended for applications with high absorptions, high linearity and low stray light:

- polarizing films
- transmission of functional films
- thickness determination of thin films
- protein and nucleic acid determination
- environmental analysis – quantification of inorganic compounds in water
- food analysis – quantification of vitamins, food additives and minerals.

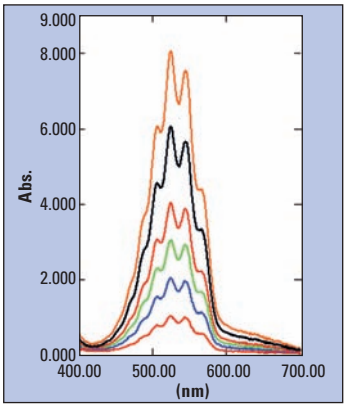

Figure 3: Measurement of a $KMnO_4$ dilution series of 8 to 1 absorption units using the UV-2700 spectrophotometer equipped with a double monochromator and LO-RAY-LIGH grating

We will gladly send you additional information. Please enter the corresponding number on the reply card or order via Shimadzu's News App or News WebApp. **Info 402**

Determination of miner vegetable oils

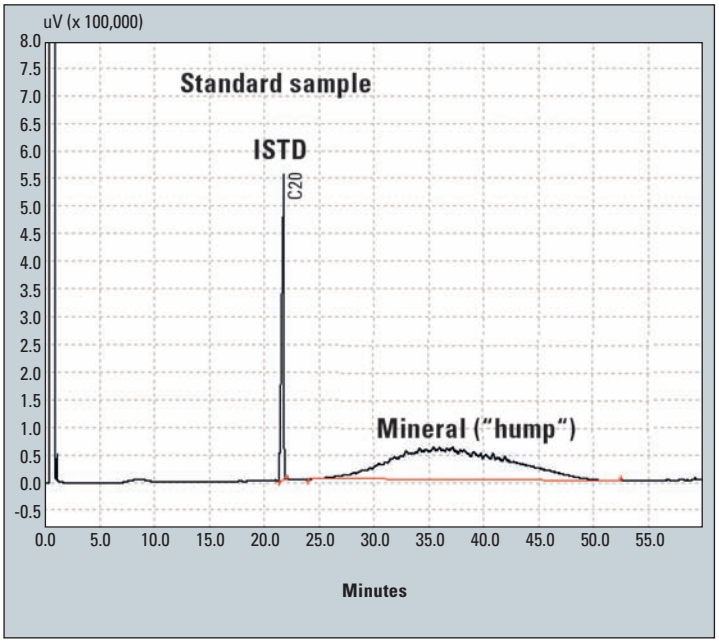

Figure 1: Chromatogram of a standard sample

Manos Barmpounis, Dimitris Georgantas
Applications Department of N.Asteriadis S.A., 31 Dervenion Str. & Poseidonos Str., 144 51 Metamorfossi – Athens, Greece,
e-mail: mb@asteriadis.gr

Vassiliki Panagiotopoulou, Vassilis Tzamtzis
GeneralChemicalState Laboratory, 16 An. Tsocha Str., 11521 Athens

Today food contamination through paraffins of mineral oil origin happens rather often. Although it is difficult to identify the exact sources of contamination, it is well known that many occur due to the wide range of applications of this petroleum derivative in many fields. Packaging additives, lubricants, cosmetics additives and pesticides can release paraffin waxes and oils. As a result, many cases of mineral oil contamination in food relating to edible oils, bakery products, packaged foods and recycled cartons are reported in literature.

The presence of mineral oils in food can produce undesired toxicological effects. Acceptable daily intakes have been established by the Joint FAO/WHO Expert Committee on Food Additives (JECFA) as 0 - 20 mg/kg body weight for high viscosity mineral oils, 0 - 10 mg/kg body weight for low and medium density class I mineral oils and 0 - 0.01 mg/kg body weight for low and medium density class II and class III mineral oils [1].

In spring 2008, nearly 100,000 t of sunflower oil were found to be contaminated in Ukraine with mineral oil at concentrations often above 1,000 mg/kg. Following this discovery, the European Commission with DG SANCO requested the national food authorities to withdraw the contaminated Ukrainian oil from the market. In June 2008, an administrative limit of 50 mg/kg was specified for mineral paraffins in crude as well as in refined Ukrainian sunflower oil.

The contaminated sunflower oil case highlights the importance of having a reliable, sensitive and simple method to determine mineral oil hydrocarbons in vegetable oils.

Principle

The saturated hydrocarbons of the sample are isolated by silica gel column chromatography and determined by capillary gas chromatography using an Internal Standard Method.

al oil hydrocarbons in

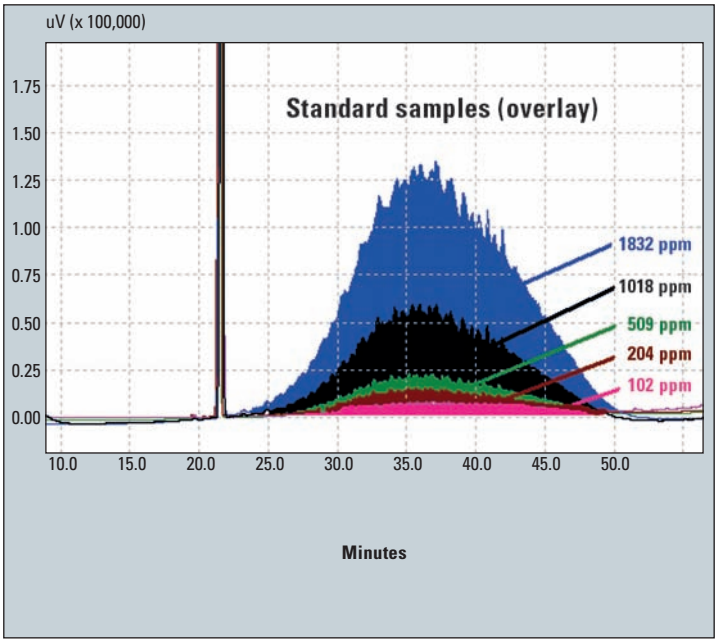

Figure 2: Chromatograms of standard samples (data comparison)

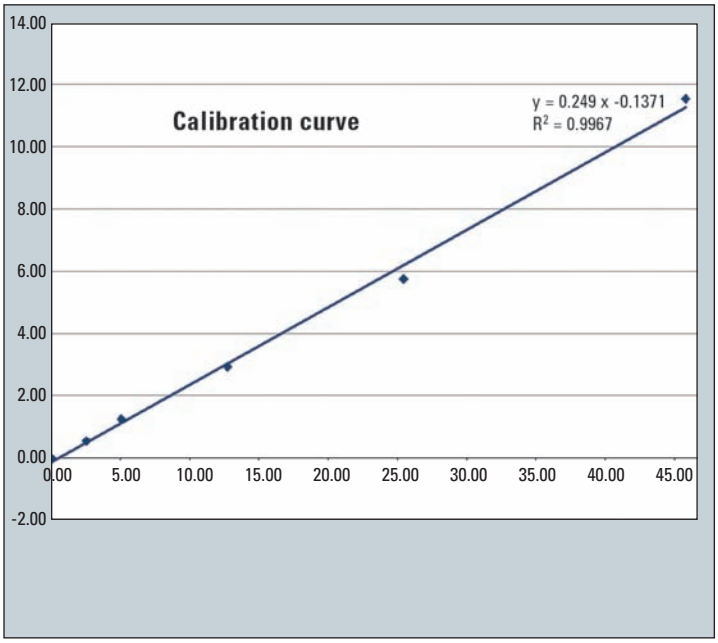

Figure 3: Calibration curve in mg/kg

Apparatus

- Erlenmeyer flasks, 25 mL
- Test tubes with glass stop
- Glass column for liquid chromatography, internal diameter (15 - 20 mm), length 30 - 40 cm, fitted with suitable frit and stop-cock

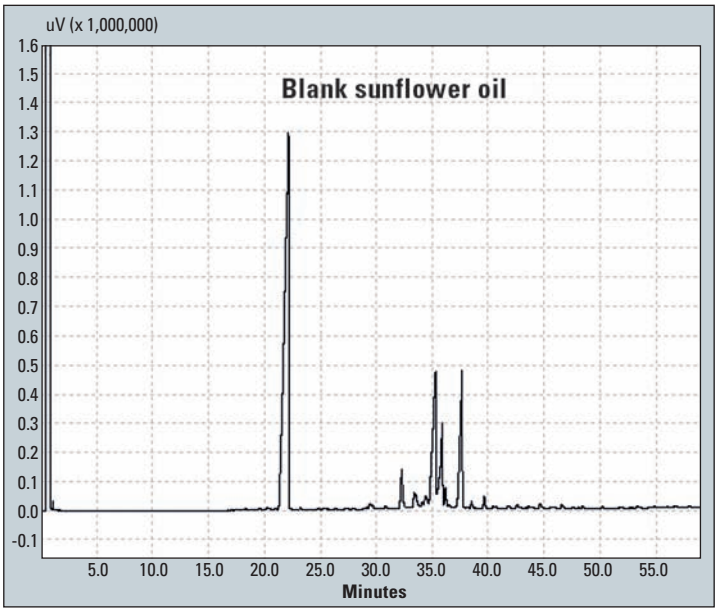

Figure 4: Chromatogram of a blank sunflower oil

- Micro-syringe for on-column injection, 10 µL, with a hardened needle
- Rotary evaporator
- Analytical balance for weighing to an accuracy of within 0.1 mg
- Usual laboratory glassware (variable volume automatic pipettes etc.)

Instrumentation

- Gas chromatograph Shimadzu GC-2010 Plus, OCI/PTV-2010 injector and FID-2010 Detector
- Capillary column (MEGA1, 10 m, 0.25 mm ID, 0.1 µm film thickness)
- Pre-column 0.53 ID 5 m deactivated (MEGA retention gap, 0.53 ID)

Temperature program

- PTV: 65 oC (5 min), 30 °C/min to 180 °C, 6 °C/min to 350 and hold 40 min
- Column Oven: 65 °C (5 min), 5 °C/min to 350 and hold 10 min
- FID temperature: 360 °C
- Total flow: 5.5 mL/min
- Carrier gas: Helium

Reagents

- Silica gel: Silica gel 60, Merck extra pure for column chromatography (code 107754). Activated at 300 °C for 24 h and cooled to room temperature in a desiccator
- n-hexane for chromatography (Unisolv by Merck is proposed).
- Internal standard, n-eicosane 20 µg/mL, by dilution from the standard 2000 µg/mL in isooctane (Neochema Cat. No 14700-0230).
- Paraffin oil, Merck, Product Number 1.07160 (for calibration curve).
- 0.2 g of paraffin oil is diluted in 100 mL of hexane, creating a 2,000 mg/L standard

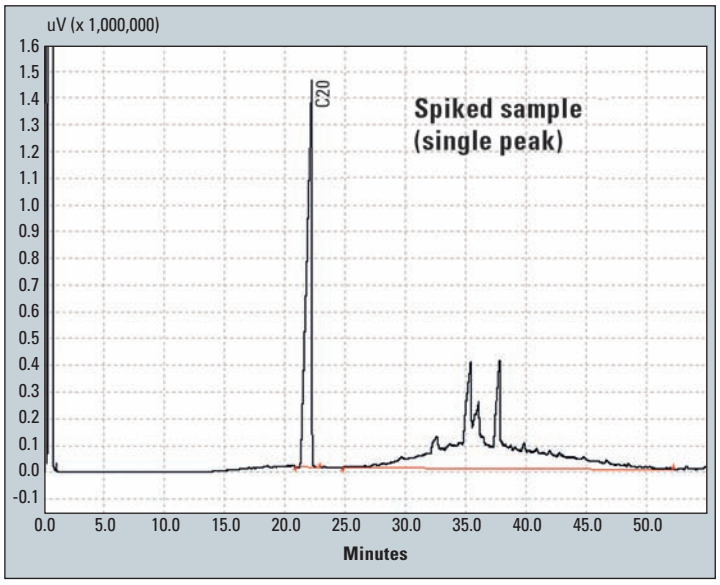

Figure 5: Chromatogram of a spiked sample integrated as single peak

Procedure – Sample pretreatment

Suspend 15 g of the above prepared silica gel in excess n-hexane, stir thoroughly with glass rod and introduce into the column. Allow to settle while gently tapping the silica by passing small quantities of n-hexane in order to make the chromatographic band more homogeneous. Weight 1 g of the sample into a 4 mL vial with screw cap, add 1 mL of the internal standard solution and mix thoroughly [2].

The sample solution should be transferred to the chromatographic column with the aid of two 1-mL portions of n-hexane. After introduction of the sample into the silica, the mineral oil hydrocarbons are eluted using 50 mL of n-hexane. Eluent flow should be set to 10 drops/15 sec. The resultant fraction is collected in a 100 mL Erlenmeyer flask and evaporated in a rotary evaporator until the solvent volume is approximately 1 mL. The rest of the solvent is removed by nitrogen stream until dryness. The isolated mineral hydrocarbons are transferred to a 2 mL autosampler vial using 500 µL of heptane.

Finally, inject 1 to 4 µL of the solution in the gas chromatograph. As can be seen in Figure 1, mineral oil hydrocarbons produce a broad unresolved peak usually referred to as "hump" [3,4,5,6] instead of forming sharp peaks in GC. The hump and the ISTD peak are integrated to create the calibration curve (Figure 3). In the case of an unknown sample, the hump and peaks are integrated as a single peak (resolved and unresolved peaks) using the manual integration bar of the GCsolution program (Figure 5).

All resolved peaks and the ISTD peak (above the hump) are then integrated using the proper drift in the GC solution program (Figure 6). Using a calculator, the area of the hump (unresolved peaks) is determined by subtracting the area of resolved peaks from the area of resolved and unresolved peaks.

The mineral concentration is calculated using the following equation:

$$c = \frac{m_{IS}}{m} \sum \frac{\frac{A_{paraf}}{A_{IS}} b}{a} \sum 1{,}000$$

where:

c = mineral concentration (mg/kg)
m = weight of the sample (g)
m_{IS} = weight of the internal standard (mg)
A_{paraf} = area of the mineral oil
A_{IS} = area of the internal standard
A = slope of the calibration curve
b = y-intercept of the line

mg/Kg	RSD %	Uncertainty % (k = 2)	Recovery
50	4	8	99 %
150	3	6	99 %

Table 1: Validation data of the method

Validation data

Two spiked samples of concentration of 50 and 150 mg/kg respectively were used. Six repetitions of each sample were performed and the results are shown in table 1. The limit of detection (LOD) was found to be 10 mg/kg and the limit of quantitation (LOQ) was found to be 20 mg/kg.

Conclusions

Mineral oil hydrocarbons were successfully determined by the above method, using a Shimadzu GC-2010 Plus gas chromatograph. The method showed good repeatability and linearity.

References

[1] JECFA (Joint FAO/WHO Expert Committee on Food Additives) (1995) Summary of Evaluations Performed by the Joint FAO/WHO Expert Committee on Food Additives www.inchem.org/documents/jecfa/jeceval/jec_1655.htm
[2] Official Method for stigmatadienes and waxes, Regulation EEC 2568/91
[3] L. Karasek, T. Wenzl, F. Ulberth, EUR 23811 EN – Joint Research Centre – Institute for Reference Materials and Measurements, Proficiency test on the determination of mineral oil in sunflower oil
[4] M. Biedermann, K. Grob, Eur. J. Lipid Sci. Technol. 111 (2009) 313-319, How "white" was the mineral oil in the contaminated Ukrainiansunflower oils?
[5] D. Fiorini, A. Paciaroni, F. Gigli, R. Ballini, Food Control 21 (2010) 1155-1160, A versatile splitless injection GC-FID method for the determination of mineral oil paraffins in vegetable oils and dried fruit
[6] K. Grob,M.Vass, M. Biedermann, H-P Neukom, Food Additives and Contaminants 18 (2001) 1-10, Contamination of animal feed and food from animal origin with mineral oil hydrocarbons

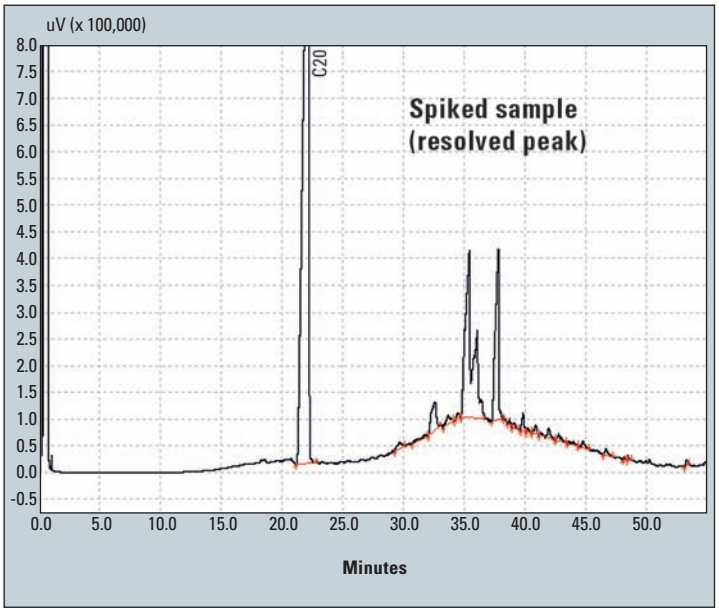

Figure 6: Integration of peaks of the spiked sample